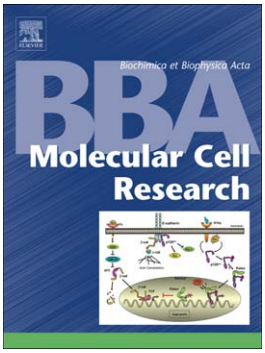

The actin binding cytoskeletal protein Moesin is involved in nuclear mRNA export

Ildikó Kristó, Csaba Bajusz, Barbara N. Borsos, Tibor Pankotai, Joseph Dopie, Ferenc Jankovics, Maria K. Vartiainen, Miklós Erdélyi, Péter Vilmos

PII: S0167-4889(17)30145-3
DOI: doi:10.1016/j.bbamcr.2017.05.020
Reference: BBAMCR 18106

To appear in: *BBA - Molecular Cell Research*

Received date: 11 November 2016
Revised date: 22 May 2017
Accepted date: 25 May 2017

Please cite this article as: Ildikó Kristó, Csaba Bajusz, Barbara N. Borsos, Tibor Pankotai, Joseph Dopie, Ferenc Jankovics, Maria K. Vartiainen, Miklós Erdélyi, Péter Vilmos, The actin binding cytoskeletal protein Moesin is involved in nuclear mRNA export, *BBA - Molecular Cell Research* (2017), doi:10.1016/j.bbamcr.2017.05.020

The actin binding cytoskeletal protein Moesin is involved in nuclear mRNA export

Ildikó Kristó[a], Csaba Bajusz[a], Barbara N. Borsos[b], Tibor Pankotai[b], Joseph Dopie[c,1], Ferenc Jankovics[a], Maria K. Vartiainen[c], Miklós Erdélyi[a], Péter Vilmos[a,*]

a Biological Research Center of the Hungarian Academy of Sciences, Szeged, Hungary

b Department of Biochemistry and Molecular Biology, University of Szeged, Szeged, Hungary

c University of Helsinki, Institute of Biotechnology, Helsinki, Finland

* Corresponding author. Tel: +36 62 599689; E-mail: vilmos.peter@mta.brc.hu.

[1] Present address: Joseph Dopie, University of Illinois, Urbana, USA

ABSTRACT

Current models imply that the evolutionarily conserved, actin-binding Ezrin-Radixin-Moesin (ERM) proteins perform their activities at the plasma membrane by anchoring membrane proteins to the cortical actin network. Here we show that beside its cytoplasmic functions, the single ERM protein of *Drosophila*, Moesin, has a novel role in the nucleus. The activation of transcription by heat shock or hormonal treatment increases the amount of nuclear Moesin, indicating biological function for the protein in the nucleus. The distribution of Moesin in the nucleus suggests a function in transcription and the depletion of mRNA export factors Nup98 or its interacting partner, Rae1, leads to the nuclear accumulation of Moesin, suggesting that the nuclear function of the protein is linked to mRNA export. Moesin localizes to mRNP particles through the interaction with the mRNA export factor PCID2 and knock down of Moesin leads to the accumulation of mRNA in the nucleus. Based on our results we propose that, beyond its well-known, manifold functions in the cytoplasm, the ERM protein of *Drosophila* is a new, functional component of the nucleus where it participates in mRNA export.

Keywords: Moesin; mRNP; PCID2; mRNA export; actin; *Drosophila*

Abbreviations: ChIP, chromatin immunoprecipitation; DMSO, Dimethyl sulfoxide; ERM, Ezrin-Radixin-Moesin; IgGH, Immunoglobulin G Heavy chain; HS, Heat Shock; LMB, Leptomycin B; LatA, Latrunculin A; Nup98, Nucleoporin98; NLS, Nuclear Localization Sequence; pAbp, polyA Binding Protein; PCID2, PCI domain-containing Protein 2; Rae1, RNA Export Factor 1; RNAPII, RNA Polymerase II; Pol2, RNA Polymerase II

1. INTRODUCTION

In the last few years, it has been shown that, besides the nuclear intermediate filament-forming lamins, several cytoskeletal components are also present in the nucleus including actin, actin-binding and -crosslinking proteins [1-4]. However, the existence of a structure mechanically and functionally analogous to the cytoskeleton in the nucleus is not known. Recently, these proteins, especially actin, actin-binding proteins (ABPs), and actin-related proteins (ARPs), receive particular attention because more and more evidence suggests that they are present in all major nuclear complexes [2,5].

We study the nuclear localization and function of Moesin (Moe), a member of the evolutionarily conserved, actin-binding ERM protein family. The main function of active ERM proteins in the cytoplasm is the crosslinking of cell membrane proteins to the cortical actin cytoskeleton. They bind various transmembrane proteins with their FERM domain and anchor them to the actin cortex through their actin-binding domain. Although this membrane-cytoskeletal linkage is critical for the stability of the cell cortex, recent studies indicate that this is only a part of what ERMs do in many cells. Up to the present, the localization and functional studies on ERMs have focused only on the cytoplasm, but our laboratory has observed that the sole ERM protein of *Drosophila melanogaster*, Moesin, is present in the nucleus as well, both in cultured cells and *in vivo* [6]. In our work presented here, we explore the biological significance of the nuclear localization of Moe. The data we display here illustrate that Moe is a functional component of the nucleus and demonstrate that it plays role in mRNA export.

2. RESULTS

2.1. Moesin localizes to the nucleus

The localization of the actin-binding Moe protein to the nucleus was observed by immunostaining for the endogenous protein in cultured S2R+ Drosophila cells (Fig 1A) as well as salivary glands of third instar larvae (Fig 1B). The V5 epitope tag and GFP-labeled Moe proteins (Moe-V5 and Moe-GFP, respectively) expressed in S2R+ cells under the control of the *actin5C* promoter (Fig 1A) or in the salivary gland by a salivary gland-specific driver (*Sgs3*>Gal4) (Fig 1B) showed the same nuclear localization in the nucleus suggesting that the presence of Moe in the nucleus is not affected by the used epitope tag. We also noted that the staining intensities in the nucleus and the cytoplasm are about the same in the confocal images. The western-blot analysis of isolated nuclear and cytoplasmic protein fractions purified from S2R+ cells further verified the existence of nuclear Moe (Fig 1C). In this experiment same amount of total protein (1 μg) of each fraction was loaded on the gel, therefore the amounts of Moe protein in the nuclear and cytoplasmic fractions could be compared in each sample (endogenous Moe, Moe-V5, Moe-GFP). This revealed that the concentrations of Moe in the two cellular compartments are about the same, supporting the observation about the similar fluorescent intensities in the nucleus and in the cytoplasm.

The salivary gland cells of *Drosophila* third instar larvae undergo multiple endoreplication cycles without cell division and, as a result, they have extremely big nuclei with giant polytene chromosomes. Live imaging of these cells revealed the fine details of the nuclear distribution of Moe: the protein is uniformly present in the nucleoplasm, enriched in some chromosome regions, and is absent from the nucleolus (Fig 1D).

2.2. The amount of nuclear Moesin is regulated

In the next set of experiments we investigated whether the protein level of Moe can be influenced in the nucleus. We stimulated salivary glands with the molting hormone ecdysone as well as heat-shock treatment. Both treatments induce high transcriptional activity in the nucleus due to the activation of specific target genes [7,8]. We found that upon one hour long heat-shock treatment at 37°C the level of nuclear Moe was significantly higher compared to the untreated control (Fig 2A). The incubation of Moe-GFP-expressing salivary glands in Drosophila Schneider's medium complemented with 20 μM Ponasterone A (ecdysone analog) had a similar

effect: nuclear Moe level was elevated following a one-hour treatment, and it was even higher after two and three hours of incubation (Fig 2B).

The Drosophila S2R+ cell line is not sensitive to ecdysone because it fails to express ecdysone receptors, but we could test the effect of heat-shock treatment on these cells by monitoring the nuclear/cytoplasmic ratio of the GFP signal after 15 and 30 minutes of heat shock in cells transiently transfected with the Moe-GFP expression vector. Compared to untreated control cells, we noticed a significant increase in the nuclear accumulation of the Moe-GFP protein which correlated with time upon 15 and 30 minutes of heat shock (Fig 2C, quantification in D). Western-blot analysis of isolated nuclear and cytoplasmic protein fractions purified from S2R+ cells further verified the increase of nuclear Moe upon heat shock (Fig 2E).

2.3. Inhibition of mRNA export induces nuclear accumulation of Moesin

Actin has a dedicated export-import system to shuttle between the nucleus and the cytoplasm [3,9-10], which supports the view that Moe might also translocate into and out of the nucleus in a regulated fashion. In order to attain deeper knowledge of the nuclear transport of Moe, we conducted an RNAi screen of all identified Drosophila cytoplasmic-nuclear transport factors [9] in cultured S2R+ cells (Table A.1). The screen revealed that the knock-down of the export factor Nucleoporin 98 (Nup98) leads to the statistically significant increase of the ratio of nuclear and cytoplasmic fluorescent intensity values of Moe-GFP (Fig A.2). Since these data were obtained by analyzing images taken with a conventional fluorescent microscope, next we visualized the effect of Nup98 depletion by a confocal microscope. This approach clearly demonstrated that the depletion of Nup98 in the cells transiently expressing Moe-GFP results in the accumulation of Moe in the nucleus (Fig 3A). To verify this finding, we silenced the mRNA export factor 1 (Rae1), a known interacting partner of Nup98 [11], in S2R+ cells expressing Moe-GFP. The knock-down of Rae1 also led to the enrichment of the Moe-GFP signal in the nucleus, corroborating that the nuclear export of Moe is dependent on Nup98/Rae1 (Fig 3A). To test whether the depletion of Nup98 or Rae1 cause a general block in nuclear export, the intracellular localization of GFP-tagged MAL (an actin-regulated SRF transcriptional coactivator [12]) was monitored in Nup98 and Rae1 depleted cells. The distribution of MAL was normal in these cells, suggesting that the effect of silencing *Nup98* or *Rae1* on the localization of Moe is not the result of the general arrest of nuclear export (Fig 3A). The depletion of Nup98 in live animals

further strengthened the idea that Nup98/Rae1 are specifically involved in the nuclear export of Moe (Fig 3B, quantification in C).

However, these results also raise the possibility that the depletion of Nup98/Rae1 leads to the nuclear accumulation of Moe not because Moe is simply exported by Nup98/Rae1 but because Moe is an active member of the mRNA export machinery. To assess whether the restriction of mRNA export causes the nuclear accumulation of other export factors, we stained for a known mRNA export factor, the PCI domain-containing Protein 2 (PCID2) which resides predominantly within the cytoplasm [13], in Rae1 depleted cells. The PCID2 protein is part of the TREX-2 mRNA export complex [14] and in *Drosophila* it was shown to participate in mRNA export from the nucleus [13]. Similarly to Moe, PCID2 became predominantly nuclear when mRNA export was suppressed (Fig 3D, quantification in E) demonstrating that the block of mRNA export leads to the accumulation of export factors in the nucleus thus supporting the idea that Moe can play a role in mRNA export. Interestingly, we observed that actin, which has been implicated in mRNA export [15-17], also accumulated in the nucleus upon Rae1 silencing (Fig 3D, quantification in E) providing additional support for the idea that Moe might be an active member of the mRNA export machinery.

2.4. Moesin is present in the transcriptionally active regions of chromosomes

As our finding of nuclear accumulation of Moe following transcriptional activation by heat shock and hormonal treatment indicated that in the nucleus Moe is most likely involved in gene expression, we decided to investigate its function in transcription. First we analyzed the localization pattern of Moe on the chromosomes by performing co-immunostaining with Moe antibody and DAPI, which marks the closed, dense chromatin, on polytene giant chromosomes from salivary glands of third instar larvae. We found that the DAPI and Moe stainings were fully complementary (Fig 4A). This finding was confirmed using the epitope-tagged forms of Moe (Moe-Myc: Fig 4B and Moe-HA: Fig 4C, quantification in G), revealing that Moe is present in the loosely packed, transcriptionally active regions of chromosomes.

To confirm the idea that Moe has a function in transcription, we tested for the presence of Moe in the chromosome puffs, which are special euchromatic regions of the polytene chromosomes with extreme high levels of transcription. The activation of target genes for example by the molting hormone ecdysone or heat shock leads to the formation of these

structures. Chromosome puffs develop at specific cytological sites: ecdysone puffs arise for instance at the 74EF and 75B, while heat shock puffs develop at the 87A and 87C chromosomal regions. After heat shock or ecdysone treatment, Moe accumulated to high levels in the corresponding puff sites both in the case of intact live nuclei (Fig 4D) and chromosome preparations from salivary gland cells (Fig 4E and F) providing additional evidence for the involvement of Moe in transcription.

In the next set of experiments we analyzed if the localization of Moe to the transcriptionally active sites indeed depends on transcriptional activity. For this aim first we employed the drug triptolide, which specifically causes the disassembly of the transcription complex through the proteasomal degradation of RNA Polymerase II (Pol2) [18], and monitored the localization of Moe to the chromosomes. Co-immunostaining of giant chromosomes for Moe and Pol2 after treatment with 1 μM triptolide for 45 minutes revealed that, similarly to Pol2, Moe fully dissociates from the chromosomes (Fig 4H) providing further evidence for the assumption that Moe is recruited to active sites to play role in gene expression.

To unambiguously demonstrate that Moe has a function in transcription, we transfected Drosophila S2R+ cells with hemagglutinin tagged Moe (Moe-HA) and measured the Moe-HA occupancy at the *Act42A* and *Hsp70* genes by using chromatin immunoprecipitation (ChIP) (Fig 4I). Specific primers for an intergenic region were used as negative control and cells expressing the HA tagged version of the chromatin binding Modigliani (DTL) protein [19] as positive control. Moe was present at the promoter region of *Act42A* but considerable level of the protein was not detected at the *Hsp70* gene. To activate the transcription of the *Hsp70* gene and silence *Act42A* at the same time, we heat shocked the cells at 37°C for 30 minutes. The treatment resulted in elevated binding of Moe at the *Hsp70* promoter as well as at the gene body while the protein exhibited untraceable association with *Act42A* (Fig 4I). Taken together these data show that Moe binds to the chromatin and its chromatin-bound level correlates with the transcriptional rate of the genes examined, thus demonstrating that Moe is involved in gene expression.

2.5. Moesin is not involved in transcription initiation or termination

Our results support a function for Moe in gene expression but how Moe performs its activity has not been characterized. To gain deeper insight into the role played by Moe in gene expression, first we aimed to identify the phase of transcription in which Moe takes part. We

directly compared the distribution of Moe along the chromosomes with the localization pattern of the active forms of Pol2 by using antibodies that recognize either the initiation-specific phosphoserine 5 (Pol2-PS5) (Fig 5A) or the elongation-specific phosphoserine 2 (Pol2-PS2) (Fig 5B) forms of Pol2. We found that Moe positive bands were often negative for Pol2-PS5 (arrowhead in Fig 5A) suggesting that Moe is not involved in initiation but rather in the later steps of transcription. In the case of Pol2-PS2, Moe was recruited to nearly all of the Pol2-PS2-positive sites, indicating that Moe participates in the elongation phase of transcription. However, we noticed that a subset of these sites exhibited only a modest signal for Moe (arrow in Fig 5B) maybe due to the fact that the antibody recognizing the phosphoserine 5 form of Pol2 marks sites of both elongation and initiation [20]. Similarly to the PS5 staining, some Moe positive bands were negative for Pol2-PS2 (arrowhead in Fig 5B). To clarify this, we carried out triple immuno-staining experiments for Moe+Pol2-PS2+Pol2-PS5 (Fig 5C, quantification in D) looking for differences in the localization intensities. The triple staining revealed that the loci exhibiting positive signal for initiation but not for elongation showed very weak or no Moesin staining (arrowheads in Fig 5C) whereas at the sites of elongation (identified by very weak or no PS5 but strong PS2 signals) the localization of Moe was clear (arrow in Fig 5C). In addition, the intensity of the Moe signal corresponds to the PS2 but not the PS5 staining intensity at chromosome sites double positive for PS2 and PS5 (marked by asterisk in Fig 5C). The quantification of the signals along an entire chromosome arm (Fig A.3) supported the finding that Moe localization correlates with the elongation and not the initiation signal, further confirming that Moe is not involved in initiation but plays a role in elongation and/or in a molecular event coupled with or following elongation (transcription termination, pre-mRNA processing, mRNA export).

To determine whether Moe participates in transcription elongation, termination, or both, we employed the well-characterized transcriptional program of the wandering third-instar larval stage [21,22]. The puff stages (PS1-8) can be identified via the morphology and the presence or absence of the ecdysone-induced puffs at specific cytological locations. We monitored these puffs at positions 74EF and 75B, whose expression is induced during this period of development, and the *Sgs3* intermolt gene at location 68C, which is turned off by ecdysone induction. The analysis of Moe recruitment to gene loci 74EF/75B and 68C during development (Fig 5E) revealed an accumulation of Moe in parallel to Pol2-PS2 enrichment as well as a loss of Moe signal when transcription terminated. These results suggest that Moe localizes to genes that are

undergoing activation, and its nuclear function is coupled to the elongation phase of transcription at the target loci.

2.6. Moesin is not involved in transcription, polyadenylation or splicing

During transcription the elongation of mRNA is associated with additional RNA processing steps such as splicing, polyadenylation and mRNP export [23]. Therefore, we wanted to examine whether Moe plays role in any of these molecular events. To test the involvement of Moe in transcription elongation, we analyzed 5-fluorouridine (5-FUrd) incorporation into nascent mRNAs. We observed that, in contrast to triptolide treatment which blocks transcription, 5-FUrd incorporation in Moe depleted cells was normal (Fig 6A, quantification in B) indicating that Moe is not required for transcription elongation. To investigate if Moe activity is needed for polyadenylation, we applied the ePAT method [24] to compare the poly(A) tail length of the heat shock inducible *Hsp83* mRNA in cells knocked down for the sole Drosophila poly(A) polymerase (*hiiragi - hrg*) [25] or Moe. We found that the poly(A) tail length was unaffected in Moe depleted cells (Fig 6C, quantification in D), suggesting that Moe is not involved in polyadenylation. Finally, to address whether Moe is an active player in RNA splicing, we analyzed the co-localization of Moe and the splicing speckles [26] in the nucleus. The co-immuno staining for endogenous Moe and the nuclear speckle marker protein, SC35 in salivary gland nuclei did not reveal any co-localization (Fig. 6E). Accordingly, the fluorescent *in situ* hybridization (FISH) experiment demonstrated that the spliced form of Hsp83 mRNA in heat shocked salivary gland cells (Fig 6F) can be detected in Moe RNAi treated cells providing additional evidence that Moe does not play role in splicing.

2.7. Moesin is part of the nuclear mRNP complexes

During the experiments, we noticed that in the chromosome preparations Moe staining also gives a punctate pattern outside the chromatin; therefore, since Moe activity seemed to be linked to transcription we examined if these dots correspond to the messenger ribonucleoprotein (mRNP) particles [27]. The double labeling of polytenic chromosome preparations for Moe and Rae1 or Moe and the poly-A Binding Protein (pAbp) confirmed that the spots Moe localizes to are in fact mRNP particles (Fig 7A). This observation together with the finding that the depletion of the mRNA export proteins Nup98 or Rae1 leads to the nuclear accumulation of Moe strongly

support the idea that in the nucleus Moe is a new member of mRNP complexes and is involved in mRNA export.

The localization of Moe to the mRNP particles prompted us to identify the interaction partner for Moe in the mRNA export complex. To this aim we performed an immuno-precipitation screen with all verified Drosophila mRNA export factors [13] and Moe. The GFP tagged Moe proteins (full-length and the FERM domain), Nup98-Myc, Rae1-FLAG, and the V5 epitope tagged PCID2, ZC3H3, l(1)10Bb, CG2063, CG2685, CG14701, CG31126 proteins were tested (Table A.2). In this experiment the physical interaction between Rae1 and Nup98 reported before [11] has been confirmed (Fig 7B), and both the full-length Moe and its FERM domain alone were successfully co-precipitated with PCID2 (Fig 7C).

To investigate if similarly to the cytoplasm, Moe can crosslink proteins to actin in the nucleus, we analyzed the localization pattern of the GFP-tagged forms of actin and the actin-binding domain (lacking the FERM and the alpha-helical regions) of Moesin (Fig 7D). We found that the localization patterns of both proteins appear identical to that of the full-length Moe (Fig 1D): uniform localization in the interchromatic space, banded pattern on the chromosomes and absence from the nucleolus. This suggests that, similarly to its activity in the cytoplasm, Moe might anchor proteins to actin in the nucleus. However, when we expressed the FERM domain (lacking the F-actin-binding motif) of Moesin we observed the same nuclear localization pattern (Fig 7D). In addition, the treatment of the cells with the F-actin severing drug, Latrunculin A did not lead to the dissociation of Moesin from the chromosomes (Fig 7E) raising the possibility that Moe is recruited to transcriptionally active sites not through F-actin binding.

2.8. Loss of Moesin inhibits nuclear mRNA export

Since our data clearly argue for a role of Moe in mRNA export, we presumed that the reduction of Moe activity impairs nuclear mRNA export. To test this, we applied FISH to monitor the subcellular relocalization of poly(A) mRNA in Moe depleted S2R+ and salivary gland cells. The distribution of poly(A) mRNA in control cells is predominantly cytoplasmic (Fig 8A and B). However, the knock down of the mRNA export factor Nup98 or the treatment with Leptomycin B, a specific inhibitor of the Crm1 nuclear export pathway, leads to the accumulation of poly(A) mRNA within the nucleus (Fig 8A and B) as revealed by the strong nuclear FISH signal. Different sites of the Moe transcript were targeted by the RNAi in the case of S2R+ cells

and the salivary glands, and in both cases the silencing of Moe resulted in the significant nuclear accumulation of poly(A) mRNA (Fig 8A and B, quantifications in C) providing evidence that the Drosophila ERM protein, Moe is member of the nuclear mRNA export system.

3. DISCUSSION

Cytoskeletal, actin-binding Ezrin-Radixin-Moesin proteins are essential for cells that have a highly organized cell cortex [28]. Accordingly, the pivotal roles ERM proteins play in epithelial integrity and cancer progression [29,30] are extensively studied. All these functions of ERMs are performed in the cytoplasm, but recent studies indicated nuclear localization of ERM proteins both in vertebrate [31-33] and invertebrate [6] organisms, yet the biological significance of this localization remained unknown.

Here we report our results which reveal that in the nucleus the primary role of the single ERM of *Drosophila melanogaster*, Moesin is the export of mRNAs and that through the interaction with PCID2, Moe is a new member of the mRNP complexes. Because we found no evidence for the involvement of Moe in other steps of mRNA formation, such as transcription, splicing or polyadenylation, we think that Moe is member of the mature mRNP complexes. This idea is supported by two recent interactome capture studies which identified the mRNA-bound proteome in mature mRNPs (containing spliced and polyadenylated mRNA) of human cells [34,35]. Among the hits they identified Ezrin [34] or all three human ERMs [35] as mRNP components.

Our co-immunoprecipitation data expose the interaction of Moesin's FERM domain with PCID2. The Drosophila PCID2 is a homologue of the human Proteasome Component Domain containing Protein 2 (HGNC:25653). In the fly, it was shown to be an mRNA export factor that also associates with translationally active complexes in the cytoplasm [13]. PCID2 binds to NXF1 (MEX67/TAP) [13] which in turn was found to interact with Nup98 [36,37]. Many binding partners have been identified for the FERM domain of ERM proteins in the cytoplasm [30], therefore it is a conceivable assumption that in the nucleus ERMs have interacting partners other than PCID2, and similarly to their function in the cytoplasm, they can serve as anchors in protein assemblies, thereby stabilizing the complex. Because the functions of ERM proteins in the cytoplasm are tightly linked to actin, it is tempting to speculate that the nuclear functions of Moe are also connected to actin. Nuclear actin has been detected in all three transcription complexes [38-40] as well as mRNP particles [15,16,41]. Our results together with data in the literature show that in the nucleus the localization patterns of actin and Moe seem to be identical, they both localize to mRNP complexes [15,16], and respond with nuclear accumulation not only to Nup98 depletion [42] but also to the inhibition of the mRNA export. These together raise the

possibility that, similarly to its cytoplasmic activity, Moe performs a structural role in the nucleus by anchoring proteins through its FERM domain to F-actin. Although the presence of F-actin in the nucleus has been unambiguously demonstrated recently [43-45], most of the nuclear activities performed by actin are still linked to its monomeric and oligomeric forms [44,46]. Correspondingly, we also found that the depolymerization of F-actin by Latrunculin A treatment does not cause the detachment of Moesin from the chromosomes, and that Moesin's FERM domain alone (lacking the F-actin binding domain) shows wild type localization pattern in the nucleus. These findings together with a report on the dual involvement of the amino-terminal domain of human Ezrin in F- and G-actin binding [47] suggest that in the nucleus Moe is not binding F-actin but oligomeric or monomeric actin forms and/or its proper nuclear localization is primarily dependent on the protein interaction of its FERM domain.

Our data demonstrate the presence of the fly ERM in the nucleus and uncover its nuclear function. The observation that under certain conditions Moe accumulates in the nucleus strengthens the notion that the nuclear transport of ERM proteins is a regulated process (Fig 9). Accordingly, multiple NLS sites were predicted in mammalian ERMs [32,33] but their nuclear localization was witnessed only in subconfluent cells and their NLS sequences were examined without the induction of nuclear import. Our previous live microscopic experiments [6] demonstrated that, at least in *Drosophila*, the nuclear Moe we see without the induction of nuclear import is engulfed into the nucleus during mitosis and that the NLS dependent nuclear import is most likely needed only if transcriptional activity is increased or mRNA export is blocked. Regarding the nuclear export of ERMs, our results indicate that Moe accompanies the mRNP to the cytoplasm. Nevertheless, in the Moe protein sequence Crm1 dependent nuclear export signals can be predicted (LocNES, http://prodata.swmed.edu/LocNES/LocNES.php) thus Moe, in theory, can leave the nucleus as a Crm1 cargo, independently from the Nup98/Rae1 mRNA export pathway. In addition, some of the mRNP components are released in the nucleus [48,49] which raises the possibility that similarly to other mRNA export factors ERM proteins might dissociate from the mRNP complex before their passage through the nuclear pore and remain in the nucleus (Fig 9).

The facts that 1) ERMs participate in many fundamental cellular processes, 2) in stress conditions, viral infection or neurodegenerative diseases actin and actin-binding proteins can accumulate in the nucleus to extreme amount [50], and 3) the activity of some transcription

factors (e.g. MAL/MRTF-A, Coronin2a or JMY) is regulated by the level of nuclear actin [51] underline the importance of our finding about the nuclear function of Moesin. We believe that our results offer a new perspective for the investigation of the ERM protein family and helps the better understanding of the biological and disease processes requiring the functions of the actin-binding ERM proteins.

4. MATERIALS AND METHODS

4.1. Fly stocks

Fly strains were maintained and crosses were carried out on standard cornmeal, yeast, sucrose Drosophila medium at 25 °C. Stocks number 6870 (w[1118]; P{Sgs3-GAL4.PD}TP1), 9256 (w; P{w[+mC]=UASp-GFP.Act57B}), 28562 (y[1] v[1]; P{TRiP.HM05048}attP2), 33378 (y[1] sc[*] v[1]; P{TRiP.HMS00252}attP2) and 9420 (UAS>pAbp-FLAG) were obtained from the Bloomington Drosophila Stock Center. The UAS>Rae1-GFP was a kind gift from Wu Chunlai (Louisiana State University, USA). The transgenic line expressing the actMoe-GFP transgene is described in [52].

To generate flies expressing full-length Moe-GFP, Moe-Myc and Moe-HA, the Moe-coding region was PCR amplified from the cDNA SD10366 (DGC Gold collection, BDGP) using the primer pair MoecDNSFw and MoecDNSRev with overhanging gateway recombination sites. (Primer sequences are summarized in Table A.3) The resulting PCR product was sequence-verified and recombined into pDONR221 plasmid then subcloned into the pPWG, pPWM and pPWH gateway (Drosophila Gateway Vector Collection) vectors. For the C-terminal tagging of Moe with the V5 epitope, the Moe cDNA reverse PCR primer was complemented with the sequence of the V5 epitope tag: MoeV5_cDNSRev. The PCR product was cloned into pDONR221 plasmid then subcloned into the pPW gateway (Drosophila Gateway Vector Collection) vector. The constructs were sequence-verified and standard Drosophila methods were used to generate transgenic flies.

4.2. Cloning of expression vectors for cell transfection

To generate FERM-Moe, Moe was amplified with the forward primer MoecDNSFw and with the reverse primer FERM-Moe_cDNSRev. The cloning and tagging with the GFP epitope was the same as in the case of the full length Moe protein constructs.

To generate FLAG tagged Rae1 protein, the Rae1-coding region was PCR amplified from the full-length cDNA LD40776 (DGC Gold cDNA Collection, BDGP) using the Rae1_cDNSFw and Rae1_cDNSRev primer pair with overhanging gateway recombination sites. The resulting PCR product was sequence-verified and recombined into pDONR221 plasmid then subcloned into the pAWF gateway (Drosophila Gateway Vector Collection) vector. To generate Myc tagged

Nup98 protein, the Nup98-coding region was PCR amplified from the full-length cDNA using the Nup98-96_cDNSFw and Nup98-96_cDNSRev primers. The resulting PCR product was sequence-verified and recombined into pDONR221 plasmid then subcloned into the pAWM gateway (Drosophila Gateway Vector Collection) vector. The V5 epitope tagged PCID2, ZC3H3, l(1)10Bb, CG2063, CG2685, CG14701, CG31126 were kindly provided by Pamela Silver (Department of Systems Biology, Harvard Medical School, USA).

4.3. Salivary gland experiments

4.3.1. Dissection and immunostaining

Dissection of third instar larvae was performed in Ringer's solution (182 mM KCl, 46 mM NaCl, 3 mM $CaCl_2$, 10 mM Tris-HCl pH 7.2); then the salivary glands were carefully placed into 4% paraformaldehyde-PBS (PFA-PBS) fixation solution for 20 min at room temperature (RT). The glands were then washed 2X with PBT (PBS+0.1% Triton-X) for 10 min. Blocking was carried out in PBT-N solution (PBT+1% BSA+5% FCS) for at least 1 h at RT. Glands were incubated with the primary antibody anti-Moe (rabbit polyclonal 1:2000, [52]), anti-V5 (1:400, Thermo Fisher R960-25), anti-GFP (1:500, Life Technologies A6455), or anti-SC35 (1:1000, Abcam ab11826) gently shaking overnight (O/N) at 4°C. After washing 2X with PBT for 10 min at RT, samples were incubated with the fluorescently labeled secondary antibody (1:600, Invitrogen Molecular Probes) supplemented with DAPI (0.2 µg/ml, Sigma-Aldrich) for 2 h in dark, at RT. Glands were mounted in 20 µl Fluoromount G medium (Southern Biotech) and imaged with a Leica TCS SP5 Confocal Microscope using a 63.0x1.40 oil objective.

4.3.2. Polytene chromosome preparation

Dissected salivary glands were fixed in 45% acetic acid-PBS for 5 min at RT then squashed on a Poly-l lysine-coated (Sigma-Aldrich P8920) slide under coverslip. The slide was dipped in liquid nitrogen, and the coverslip was immediately removed with a blade. Blocking and immunostaining was carried out in humidity chamber as described above. Primary antibodies were: anti-Moe (1:1000, (rabbit polyclonal [52]), anti-HA (1:200, Roche 12CA5), anti-Polymerase II CTD (phosopho-serine2, 1:200, Abcam ab5095; phospho-serine5, 1:200, Abcam ab5131), anti-Myc (1:200, Santa Cruz Biotechnology 9E10), anti-Polymerase II CTD (1:1, phospho-serine2, CTD7 3E10), anti-GFP (1:500, Life Technologies A6455), anti-FLAG M2

(1:500, Sigma-Aldrich F1804), anti-HA (1:100, Sigma-Aldrich GW22511), DAPI (0.2 µg/ml, Sigma-Aldrich). After washing 2X with 300 mM NaCl containing 0.2% Tween-20 for 10 min at RT, samples were incubated with the fluorescently labeled secondary antibody (1:600, Invitrogen Molecular Probes) for 2 h in dark, at RT. Squash preparations were mounted in 20 µl Fluoromount G medium (Southern Biotech) and imaged with a Leica TCS SP5 Confocal Microscope using a 63.0x1.40 oil objective.

4.3.3. Live imaging

Dissected salivary glands were placed into a 35 mm glass bottom dish (Cell E&G) containing Drosophila Schneider's medium (Lonza) complemented with 10% FBS (Whittaker). Glands were imaged using the 63.0x1.40 oil objective of the Leica TCS SP5 confocal microscope.

4.3.4. Drug treatments

Dissected salivary glands were placed into 1.5 ml Eppendorf tubes containing 1 µM triptolide (Calbiochem, 645900), 50 nM LMB (Sigma-Aldrich), 20 µM Ponasteron A (Cayman Chemical) or 4 µM Latrunculin A (Sigma-Aldrich L5163) in Drosophila Schneider's medium (Lonza) for 30 min (LMB), 45 min (triptolide), 1h (LatA) or 1-3h (PonasteronA).

4.3.5. FISH

Dissected salivary glands were fixed in 4% PFA-PBS for 10 min then post-fixed in methanol for 10 min, and rehydrated in 70% ethanol for 10 min. Samples were then washed in 1 M Tris (pH 8.0) for 5 min, then hybridized for 1 h at 37°C with a Cy3-Oligo-dT(30) probe (Integrated DNA Technologies) at 1 µg/ml in hybridization buffer (25% formamide, 10% dextran sulfate, 0.005% BSA, 0.4 µg/µl yeast total RNA in 2XSSC). After two washes in 2XSSC (300 mM NaCl, 30 mM Trisodium citrate, pH 7.0) for 2 min, the glands were incubated for 30 min at RT in DAPI solution (0.2 µg/ml in 2XSSC). Samples were washed 2X in 2XSSC for 2 min, placed on a microscope slide, embedded into Fluoromount-G medium (Southern Biotech) and covered with a coverslip for imaging. Images were taken with an OLYMPUS Fluoview FV1000 confocal microscope using an Olympus UPlanSApo 60X/1.35 Oil objective lens and the 60 Olympus FV10-ASW (Ver. 01.07.01.00, Olympus Corp.) software.

4.3.6. Heat-shock treatment

Third instar larvae were placed into 1.5 ml Eppendorf tubes and incubated in a 37 °C water bath for 30 min (Fig 4F, 6C, 6F) or 1 h (Fig 2A); then the salivary glands were immediately dissected for further experiments.

4.3.7. Transcription assay

Dissected salivary glands were placed into 1.5 ml Eppendorf tubes for triptolide or control (DMSO/water) treatments as described above. Then the glands were placed into Drosophila Schneider's medium supplemented with 2 mM 5-Fluorouridine (Sigma, F5130) and incubated for 20 min at RT. After washing with complete medium, the samples were fixed, immunostained and imaged as described above. Primary antibody was anti-BrdU (1:500, B2531 Sigma).

4.3.8. Splicing test

Third instar larvae were heat-shock treated, then the salivary glands were dissected, fixed and a Cy3 conjugated FISH probe specific to the spliced form of Hsp83 mRNA (Hsp83_Spliced, Integrated DNA Technologies) was applied. Conditions of FISH protocol and imaging were as described above.

4.3.9. Extension Poly(A) Test (ePAT)

Total RNA was isolated from salivary glands of heat shocked third instar larvae, 50/genotype by using the TRIzol (Invitrogen, 15596-018) method. We followed the ePAT protocol as described in [23] with some modifications: we purchased the reverse transcriptase enzyme from Invitrogen (SuperScript IV, 18090010) and the Klenow enzyme from Fermentas (EP0051). The gene specific primer for the Hsp83 mRNA was Hsp83_PAT (Integrated DNA Technologies).

4.4. Cell culturing

4.4.1. S2R+ cell maintenance, transfection, RNAi treatment and immunostaining

The S2R+ *Drosophila* cell line was maintained in Schneider's Drosophila medium (Lonza) complemented with 10% Fetal Bovine Serum (Whittaker) and 1% antibiotics (Penicillin-Streptomycin, Gibco) at 25°C. To transfect the cells, we used the Effectene Transfection Reagent Kit (Qiagen, Cat. No.: 301425) and followed the manufacturer's instructions. For protein

expression $2x10^5$ cells/well (24-well plate, Greiner), $2x10^6$ cells/petri dish (60 mm, Nunclon) or $1x10^6$ cells/petri dish (35 mm glass bottom dish, Cell E&G) and 2 days of incubation after transfection were used. In the RNAi experiments $1.5x10^5$ cells/well (24-well plate, Greiner), $1.7x10^6$ cells/petri dish (60 mm, Nunclon) or $0.8x10^6$ cells/petri dish (35 mm, glass bottom dish, Cell E&G) and 5 days of incubation after transfection were used.

For RNAi experiments, PCR was performed on S2R+ cDNA template with target gene specific primers containing the T7 promoter sequence. The PCR product was used in the *in vitro* transcription assay (MEGAscript T7 transcription Kit, AM1334) according to the manufacturer instructions. Template DNA was digested, and the dsRNA was isolated (NucAway Spin Columns, AM10070). For Nup98 and Rae1 silencing two independent dsRNAs were used with different target sites. Cells adhered to round glass coverslips were fixed in 4% PFA-PBS, immunostained and mounted as described previously then imaged with a Leica TCS SP5 confocal microscope using a 63.0x1.40 oil objective. The primary antibodies and dilutions were: anti-Moe (rabbit polyclonal 1:2000, [52]), anti-GFP (1:500, Life Technologies A6455), anti-V5 (1:400, Thermo-Fisher R960-25). Samples were incubated with the fluorescently labeled secondary antibody (1:600, Invitrogen Molecular Probes) and DAPI (0.2 µg/ml, Sigma-Aldrich) for 2 h in dark, at RT. In the RNAi screen, images were taken using a Zeiss Axio Imager M2 microscope with a 63.0x1.40 objective.

4.4.2. Heat-shock treatments

The 24-well plate containing S2R+ cells was carefully placed in a 37°C water bath for 15 or 30 min; then the cells were immediately fixed in 4% PFA-PBS for subsequent experiments.

4.4.3. FISH

$2x10^5$ cells were plated into the wells of a 24-well plate containing round coverslips of 12 mm diameter. On the fifth day after transfection with or without 0.2 µg of Nup98 and Moe dsRNA, the cells were fixed and stained for poly(A) mRNA as described for the salivary glands. After the last washing step the coverslips were removed from the plate, turned into a drop of Fluoromount-G medium (Southern Biotech) on a microscope slide and imaged with a Leica TCS SP5 confocal microscope.

4.4.5. Isolation of cytoplasmic and nuclear protein fractions

Cells were trypsinized, collected by centrifugation, and the pellet was washed 2X with ice-cold PBS then resuspended in Harvest Buffer (10 mM HEPES pH 7.9, 50 mM NaCl, 0.5 M Sucrose, 0.1 mM EDTA, 0.5% Triton X-100) containing freshly added proteinase inhibitor cocktail (Protease Inhibitor Cocktail Tablets, Roche #04 693 124 001), and incubated on ice for 5 min then centrifuged for 10 min with 800 g. The supernatant was transferred into a new Eppendorf tube (later this supernatant was centrifuged for 10 min at 14.000 g and used as the cytoplasmic protein fraction). The pellet was resuspended in ice-cold Buffer A (10 mM HEPES pH 7.9, 10 mM KCl, 0.1 mM EDTA, 0.1 mM EGTA, and freshly added protease inhibitor cocktail) and spun for 10 min at 800 g. The supernatant was discarded and the pellet was resuspended in ice-cold Buffer C (10 mM HEPES pH 7.9, 500 mM NaCl, 0.1 mM EDTA, 0.1 mM EGTA, 0.1% NP-40, and freshly added protease inhibitor cocktail). The sample was incubated on ice for 30 min and vortexed periodically then centrifuged for 10 min with 14,000 g; the supernatant was used as the nuclear protein fraction.

4.4.6. Western-blot

Before loading the samples on the gel, 1 µl beta-mercaptoethanol was added and the samples were boiled for 5 min and spun for 5 min with 12.000 rpm at RT. 10% acrylamide gel was used; the proteins were transferred O/N to PVDF membrane (Millipore Transfer Membranes Immobilon-P, Cat.no.: IPVH00010 PVDF 0.45 µm) using 35 mV at 4°C. Blocking was performed in 5% milk powder-TBST (25 mM Tris, 150 mM NaCl, pH 7.5+0.1% Tween-20) for 3 h and then the membrane was incubated with the primary antibodies anti-Moe (rabbit polyclonal, 1:10,000, [52]), anti-HP1 (1:200, DSHB C1A9), anti-Beta-Tubulin (1:200, DSHB E7), guinea pig anti-GFP (1:5000, [53]), anti-V5 (1:5000, Thermo Fisher R960-25), anti-FLAG M2 (1:1000, Sigma-Aldrich F1804), anti-Myc (1:500, Santa Cruz 9E10 sc-40) O/N at 4°C. The membrane was washed 2X in TBST for 20 min and incubated with the HRP-conjugated secondary antibody for 50 min. After washing 3 times for 30 min with TBST at RT, the signal was visualized using HRP Substrate solution (Millipore Immobilon Western Chemiluminescent HRP Substrate, Cat. No.: WBKLS01000) and the films were developed.

4.4.7. Protein Co-Immunoprecipitation

Cells grown in Petri dishes of 60 mm diameter were trypsinized and collected by centrifugation. The pellet was washed 2X with ice-cold PBS then resuspended in 100 µl Lysis Buffer (20 mM Tris pH 7.5, 200 mM NaCl, 10% Glycerol, 0.5 mM EDTA, 0.5% NP-40) with freshly added proteinase inhibitor cocktail, and incubated on ice for 1 h. For lysis control, 1% or 10% of the protein samples were saved. Total protein concentration was measured with the Bradford method (Pierce Coomassie Plus Assay Kit, Thermo Fisher 23236) by comparing to BSA protein standards. Equal protein amounts were calculated for the no antibody control (NAC) and immunoprecipitation (IP) samples. NAC and IP samples were diluted with Lysis Buffer then the antibody was added to the IP samples (0.5 µl monoclonal mouse anti-FLAG M2 (Sigma-Aldrich F1804) or 0.5 µl anti V5 antibody (Thermo Fisher R960-25). After gently rotation at 4°C O/N, 20 µl of Protein G magnetic beads (BioRad 161-4021) were added which were previously washed with Lysis Buffer. Samples were rotated for 1 h 15 min at 4°C, then the beads were washed with Lysis Buffer and the proteins were eluted with 300 µl of 6 M guanidine hydrochloride (Sigma-Aldrich) and precipitated by adding 700 µl water and 1 ml 20% trichloroacetic acid. After 15 min centrifugation at 4°C the protein pellet was washed with 96% Ethanol and resuspended in 2x protein SDS buffer (120 mM Tris, pH 6.8, 12.8% glycine, 4% SDS, 200 mM DTT, 0.2% bromophenol blue).

4.5. Quantification of nuclear accumulation

Pixel intensities were measured in equal cytoplasmic and nuclear areas with the ImageJ software and the nuclear/cytoplasmic ratio was calculated. The GraphPad Prism 5 software and unpaired t-test were used for the statistical analysis.

4.6. Chromatin Immunoprecipitation

Chromatin samples were prepared from S2R+ cells which were transiently transfected with Moe-HA or HA-DTL or empty expression vector pAWH. Chromatin samples were cross-linked with 1% formaldehyde (Sigma-Aldrich) for 20 min then the reaction was stopped by using 125 mM glycine (Sigma-Aldrich). Cells were collected by centrifugation (400 g, 5 min, 4 °C) and the pellets were resuspended in Cell lysis buffer [5 mM PIPES (Sigma-Aldrich) pH 8.0, 85 mM KCl (Sigma-Aldrich), 0.5% NP-40 (IGEPAL) (Sigma-Aldrich), 1XPIC (Calbiochem)]. Nuclei were collected by centrifugation (400 g, 5 min, 4 °C) and the pellets were resuspended in Nuclear lysis

buffer [50 mM Tris–HCl pH 8 (Sigma-Aldrich), 10 mM EDTA pH 8 (Sigma-Aldrich), 0.8% SDS (Sigma-Aldrich), 1XPIC (Calbiochem)] and incubated on ice for 1 h. Chromatin samples were fragmented by sonication in a Bioruptor (Diagenode) and diluted to four-fold by using Dilution buffer [10 mM Tris–HCl pH 8.0 (Sigma-Aldrich), 0.5 mM EGTA pH 8.0 (Sigma-Aldrich), 1% Triton-X-100 (Sigma-Aldrich), 140 mM NaCl (Sigma-Aldrich), 1XPIC (Calbiochem)]. 30 μg of chromatin was used for each immunoprecipitation after pre-clearing with Sheep anti-Rabbit and Sheep anti-Mouse IgG Dynabeads (Novex). Immunoprecipitations were incubated O/N at 4 °C with anti-Hemagglutinin antibody (Roche, 12CA5), then chromatin-antibody complexes were collected with Sheep anti-Rabbit and Sheep anti-Mouse IgG Dynabeads (Novex) at 4 °C, O/N. After washing steps the samples were reverse cross-linked and the amount of extracted DNA was determined by qPCR using SYBR Green PCR Master Mix (Fermentas) in Thermo PikoReal 96 Real-Time PCR System (Thermo Fisher Scientific). The primers used in the qPCR reactions were: Act42a_fwd, Act42a_rev, Hsp70Bb promoter_fwd, Hsp70Bb promoter_rev, Hsp70Bb gene body_fwd, Hsp70Bb gene body_rev, Intergenic region_fwd and Intergenic region_rev (Table A.3). The ChIP signals were normalized by using total input control percentage (TIC%) and to the amount of DNA in the no antibody sample (NAC).

AUTHOR CONTRIBUTIONS

Conceived and designed the experiments: IK, MKV, TP, PV. Performed the experiments: IK, JD, CsB, BNB, TP, FJ. Analyzed the data: IK, FJ, ME, PV. Wrote the paper: IK, ME, PV.

COMPETING INTERESTS

The authors declare that they have no conflict of interest.

ACKNOWLEDGMENTS

We thank Henrik Gyurkovics and Izabella Bajusz (BRC Szeged, Hungary) for helpful discussions, József Demeter (Merck Kft., Hungary) for the triptolide reagent, Dirk Eick (Helmholtz Zentrum, München, Germany) for the rat anti Pol2-Ser2P (3E10) antibody, Daniel Kiehart (Duke University, Durham, NC, USA) for the anti-Moe antibody, Pamela Silver (Harvard Medical School, USA) for the constructs to express tagged mRNA export factors, and Cordula Schulz (Univ. Georgia, USA) for the full-length Nup98 cDNA. Stocks obtained from the Bloomington Drosophila Stock Center (NIH P40OD018537) were used in this study.

FUNDING

This work was supported by the National Research, Development and Innovation Office – NKFIH (GINOP-2.3.2-15-2016-00001, GINOP-2.3.2-15-2016-00032, PD112118 and K117010). TP was supported by the János Bolyai Research Scholarship of the Hungarian Academy of Sciences. The research was supported also by the European Union and the State of Hungary, co-financed by the European Social Fund in the framework of TÁMOP-4.2.4.A/ 2-11/1-2012-0001 ‘National Excellence Program’.

REFERENCES

[1] D.N. Simon, K.L. Wilson, The nucleoskeleton as a genome-associated dynamic 'network of networks'. Nat Rev Mol Cell Biol 12(11) (2011) 695-708. doi: 10.1038/nrm3207

[2] I. Kristó, I. Bajusz, Cs. Bajusz, P. Borkúti, P. Vilmos, Actin, actin-binding proteins, and actin-related proteins in the nucleus. Review paper. Histochem Cell Biol. 145(4) (2016) 373-88. doi: 10.1007/s00418-015-1400-9

[3] M. Kumeta, S.H. Yoshimura, J. Hejna, K. Takeyasu, Nucleocytoplasmic shuttling of cytoskeletal proteins: molecular mechanism and biological significance. Int J Cell Biol 2012 (2012) 494902. doi: 10.1155/2012/494902

[4] E.K. Rajakylä, M.K. Vartiainen, Rho, nuclear actin, and actin-binding proteins in the regulation of transcription and gene expression. Small GTPases. (2014)5:e27539. doi: 10.4161/sgtp.27539

[5] N. Visa, P. Percipalle, Nuclear functions of actin. Cold Spring Harb Perspect Biol 2(4):a (2010) 000620. doi: 10.1101/cshperspect.a000620

[6] P. Vilmos, F. Jankovics, M. Szathmári, T. Lukácsovich, L. Henn, M. Erdélyi, Live imaging reveals that the Drosophila actin-binding ERM protein, Moe, co-localizes with the mitotic spindle. Eur J Cell Biol 88(10) (2009) 609-19. doi: 10.1016/j.ejcb.2009.05.006

[7] S. Michaud, R. Marin, R.M. Tanguay, Regulation of heat shock gene induction and expression during Drosophila development. Cell Mol Life Sci 53(1) (1997) 104-13.

[8] T.R. Li, K.P. White, Tissue-specific gene expression and ecdysone-regulated genomic networks in Drosophila. Dev Cell 5(1) (2003) 59-72.

[9] J. Dopie, K.P. Skarp, E.K. Rajakylä, K. Tanhuanpää, M.K. Vartiainen, Active maintenance of nuclear actin by importin 9 supports transcription. Proc Natl Acad Sci USA. 109(9) (2012) E544-52. doi: 10.1073/pnas.1118880109.

[10] G. Huet, K.P. Skarp, M.K. Vartiainen, Nuclear actin levels as an important transcriptional switch. Transcription 3(5) (2012) 226-30. doi: 10.4161/trns.21062

[11] M.B. Blevins, A.M. Smith, E.M. Phillips, M.A. Powers, Complex formation among the RNA export proteins Nup98, Rae1/Gle2, and TAP. J Biol Chem 278(23) (2003) 20979-88.

[12] E.N. Olson, A. Nordheim, Linking actin dynamics and gene transcription to drive cellular motile functions. Nat Rev Mol Cell Biol 11(5) (2010) 353-65. doi: 10.1038/nrm2890.

[13] N.G. Farny, J.A. Hurt, P.A. Silver, Definition of global and transcript-specific mRNA export pathways in metazoans. Genes Dev 22(1) (2008) 66-78.

[14] D. Jani, S. Lutz, E. Hurt, R.A. Laskey, M. Stewart, V.O. Wickramasinghe, Functional and structural characterization of the mammalian TREX-2 complex that links transcription with nuclear messenger RNA export. Nucleic Acids Res 40(10) (2012) 4562-73. doi: 10.1093/nar/gks059

[15] K. Maundrell, K. Scherrer, Characterization of pre-messenger-RNA-containing nuclear ribonucleoprotein particles from avian erythroblasts. Eur J Biochem. 99(2) (1979) 225-38.

[16] W. Hofmann, B. Reichart, A. Ewald, E. Müller, I. Schmitt, R.H. Stauber, F. Lottspeich, B.M. Jockusch, U. Scheer, J. Hauber, M.C. Dabauvalle, Cofactor requirements for nuclear export of Rev response element (RRE)- and constitutive transport element (CTE)-containing retroviral RNAs. An unexpected role for actin. J Cell Biol. 152(5) (2001) 895-910.

[17] P. Percipalle, J. Zhao, B. Pope, A. Weeds, U. Lindberg, B. Daneholt, Actin bound to the heterogeneous nuclear ribonucleoprotein hrp36 is associated with Balbiani ring mRNA from the gene to polysomes. J Cell Biol 153(1) (2001) 229-36.

[18] Y. Wang, J.J. Lu, L. He, Q. Yu, Triptolide (TPL) inhibits global transcription by inducing proteasome-dependent degradation of RNA polymerase II (Pol II). PLOS One 6(9) (2011) e23993. doi: 10.1371/journal.pone.0023993

[19] O. Komonyi, G. Pápai, I. Enunlu, S. Muratoglu, T. Pankotai, D. Kopitova, P. Maróy, A. Udvardy, I. Boros, DTL, the Drosophila homolog of PIMT/Tgs1 nuclear receptor coactivator-interacting protein/RNA methyltransferase, has an essential role in development. J Biol Chem. 280(13) (2005) 12397-404.

[20] J.P. Hsin, J.L. Manley, The RNA polymerase II CTD coordinates transcription and RNA processing. Genes Dev 26(19) (2012) 2119-37. doi: 10.1101/gad.200303.112.

[21] M. Ashburner, Patterns of puffing activity in the salivary gland chromosomes of Drosophila. I. Autosomal puffing patterns in a laboratory stock of Drosophila melanogaster. Chromosoma 21(4) (1967) 398-428.

[22] M. Capelson, Y. Liang, R. Schulte, W. Mair, U. Wagner, M.W. Hetzer, Chromatin-bound nuclear pore components regulate gene expression in higher eukaryotes. Cell 140(3) (2010) 372-83. doi: 10.1016/j.cell.2009.12.054

[23] M. Müller-McNicoll, K.M. Neugebauer, How cells get the message: dynamic assembly and function of mRNA-protein complexes. Nat Rev Genet. 14(4) (2013) 275-87. doi: 10.1038/nrg3434

[24] A. Jänicke, J. Vancuylenberg, P.R. Boag, A. Traven, T.H. Beilharz, ePAT: a simple method to tag adenylated RNA to measure poly(A)-tail length and other 3' RACE applications. RNA 18(6) (2012) 1289-95. doi: 10.1261/rna.031898.111

[25] T. Murata, H. Nagaso, S. Kashiwabara, T. Baba, H. Okano, K.K. Yokoyama, The *hiiragi* gene encodes a poly(A) polymerase, which controls the formation of the wing margin in *Drosophila melanogaster*. Dev Biol 233(1) (2001) 137-47.

[26] D.L. Spector, A.I. Lamond, Nuclear speckles. Cold Spring Harb Perspect Biol. 3(2) (2011) pii: a000646. doi: 10.1101/cshperspect.a000646.

[27] Y. Ji, A.V. Tulin, Poly(ADP-ribosyl)ation of heterogeneous nuclear ribonucleoproteins modulates splicing. Nucleic Acids Res 37(11) (2009) 3501-13. doi: 10.1093/nar/gkp218

[28] R.G. Fehon, A.I. McClatchey, A. Bretscher, Organizing the cell cortex: the role of ERM proteins. Nat Rev Mol Cell Biol 11(4) (2010) 276-87. doi: 10.1038/nrm2866

[29] J. Clucas, F. Valderrama, ERM proteins in cancer progression. J Cell Sci 127(Pt 2) (2014) 267-75. doi: 10.1242/jcs.133108

[30] D.C. Bosanquet, L. Ye, K.G. Harding, W.G. Jiang, FERM family proteins and their importance in cellular movements and wound healing (review). Int J Mol Med 34(1) (2014) 3-12. doi: 10.3892/ijmm.2014.1775

[31] J. Bergquist, J. Gobom, A. Blomberg, P. Roepstorff, R. Ekman, Identification of nuclei associated proteins by 2D-gel electrophoresis and mass spectrometry. J Neurosci Methods 109(1) (2001) 3-11.

[32] C.L. Batchelor, A.M. Woodward, D.H. Crouch, Nuclear ERM (ezrin, radixin, Moe) proteins: regulation by cell density and nuclear import. Exp Cell Res 296(2) (2004) 208-22.

[33] R. Krawetz, G.M. Kelly, Moe signalling induces F9 teratocarcinoma cells to differentiate into primitive extraembryonic endoderm. Cellular signaling 20 (2008) 163-175.

[34] A.G. Baltz, M. Munschauer, B. Schwanhäusser, A. Vasile, Y. Murakawa, M. Schueler, N. Youngs, D. Penfold-Brown, K. Drew, M. Milek, E. Wyler, R. Bonneau, M. Selbach, C. Dieterich, M. Landthaler, The mRNA-bound proteome and its global occupancy profile on protein-coding transcripts. Mol Cell 46(5) (2012) 674-90. doi: 10.1016/j.molcel.2012.05.021

[35] A. Castello, B. Fischer, K. Eichelbaum, R. Horos, B.M. Beckmann, C. Strein, N.E. Davey, D.T. Humphreys, T. Preiss, L.M. Steinmetz, J. Krijgsveld, M.W. Hentze, Insights into RNA biology from an atlas of mammalian mRNA-binding proteins. Cell 149(6) (2012) 1393-406. doi: 10.1016/j.cell.2012.04.031

[36] A. Bachi, I.C. Braun, J.P. Rodrigues, N. Panté, K. Ribbeck, C. von Kobbe, U. Kutay, M. Wilm, D. Görlich, M. Carmo-Fonseca, E. Izaurralde, The C-terminal domain of TAP interacts with the nuclear pore complex and promotes export of specific CTE-bearing RNA substrates. RNA 6(1) (2000) 136-58.

[37] L. Lévesque, Y.C. Bor, L.H. Matzat, L. Jin, S. Berberoglu, D. Rekosh, M.L. Hammarskjöld, B.M. Paschal, Mutations in tap uncouple RNA export activity from translocation through the nuclear pore complex. Mol Biol Cell 17(2) (2006) 931-43.

[38] W.A. Hofmann, L. Stojiljkovic, B. Fuchsova, G.M. Vargas, E. Mavrommatis, V. Philimonenko, K. Kysela, J.A. Goodrich, J.L. Lessard, T.J. Hope, P. Hozak, P. de Lanerolle, Actin is part of pre-initiation complexes and is necessary for transcription by RNA polymerase II. Nat Cell Biol 6(11) (2004) 1094-101.

[39] P. Hu, S. Wu, N. Hernandez, A role for beta-actin in RNA polymerase III transcription. Genes Dev 18(24) (2004) 3010-5.

[40] V.V. Philimonenko, J. Zhao, S. Iben, H. Dingová, K. Kyselá, M. Kahle, H. Zentgraf, W.A. Hofmann, P. de Lanerolle, P. Hozák, I. Grummt, Nuclear actin and myosin I are required for RNA polymerase I transcription. Nat Cell Biol 6(12) (2004) 1165-72.

[41] P. Percipalle, A. Jonsson, D. Nashchekin, C. Karlsson, T. Bergman, A. Guialis, B. Daneholt, Nuclear actin is associated with a specific subset of hnRNP A/B-type proteins. Nucleic Acids Res 30(8) (2002) 1725-34.

[42] J. Dopie, E.K. Rajakylä, M.S. Joensuu, G. Huet, E. Ferrantelli, T. Xie, H. Jäälinoja, E. Jokitalo, M.K. Vartiainen, Genome-wide RNAi screen for nuclear actin reveals a network of cofilin regulators. J Cell Sci. 128(13) (2015) 2388-400. doi: 10.1242/jcs.169441.

[43] K. Miyamoto, V. Pasque, J. Jullien, J.B. Gurdon, Nuclear actin polymerization is required for transcriptional reprogramming of Oct4 by oocytes. Genes Dev 25(9) (2011) 946-58. doi: 10.1101/gad.615211

[44] R. Grosse, M.K. Vartiainen, To be or not to be assembled: progressing into nuclear actin filaments. Nat Rev Mol Cell Biol 14(11) (2013) 693-7. doi: 10.1038/nrm3681

[45] M. Plessner, M. Melak, P. Chinchilla, C. Baarlink, R. Grosse, Nuclear F-actin formation and reorganization upon cell spreading. J Biol Chem 290(18) (2015) 11209-16. doi: 10.1074/jbc.M114.627166

[46] P. de Lanerolle, L. Serebryannyy, Nuclear actin and myosins: life without filaments. Nat Cell Biol 13(11) (2011) 1282-8. doi: 10.1038/ncb2364

[47] C. Roy, M. Martin, P. Mangeat, A dual involvement of the amino-terminal domain of ezrin in F- and G-actin binding. J Biol Chem 272(32) (1997) 20088-95

[48] N. Iglesias, E. Tutucci, C. Gwizdek, P. Vinciguerra, E. Von Dach, A.H. Corbett, C. Dargemont, F. Stutz, Ubiquitin-mediated mRNP dynamics and surveillance prior to budding yeast mRNA export. Genes Dev 24(17) (2010) 1927-38. doi: 10.1101/gad.583310

[49] J. Katahira, Nuclear Export of Messenger RNA. Genes 6 (2015) 163-184. doi:10.3390/genes6020163

[50] L. Munsie, N. Caron, R.S. Atwal, I. Marsden, E.J. Wild, J.R. Bamburg, S.J. Tabrizi, R. Truant, Mutant huntingtin causes defective actin remodeling during stress: defining a new role for transglutaminase 2 in neurodegenerative disease. Hum Mol Genet 20(10) (2011) 1937-51. doi: 10.1093/hmg/ddr075

[51] K. Miyamoto, J.B. Gurdon, Transcriptional regulation and nuclear reprogramming: roles of nuclear actin and actin-binding proteins Cell Mol Life Sci 70(18) (2013) 3289-302. doi: 10.1007/s00018-012-1235-7

[52] Edwards KA, Demsky M, Montague RA, Weymouth N, Kiehart DP. GFP-Moe illuminates actin cytoskeleton dynamics in living tissue and demonstrates cell shape changes during morphogenesis in Drosophila. Dev Biol 191 (1997) 103-117.

[53] S. Takáts, P. Nagy, Á. Varga, K. Pircs, M. Kárpáti, K. Varga, A.L. Kovács, K. Hegedűs, G. Juhász, Autophagosomal Syntaxin17-dependent lysosomal degradation maintains neuronal function in Drosophila. J Cell Biol. 201(4) (2013) 531-9. doi: 10.1083/jcb.201211160

FIGURE LEGEND

Fig. 1. Moesin is present in the nucleus. (A) Moe localizes to the nuclei (encircled and arrows) of Drosophila S2R+ cells as revealed by immunostaining for the endogenous protein (Moe - magenta) and the detection of the V5-tagged Moe (Moe-V5 - magenta) or Moe-GFP (Moe-GFP - green). DAPI – blue, scale bar 25 μm. (B) Similarly to cultured cells, the immuno-staining for the endogenous (Moe - magenta) and the V5- or GFP-tagged (Moe-V5 –magenta, Moe-GFP - green) Moe proteins demonstrate that all forms of Moe localize to the nuclei of salivary gland cells. DAPI – blue, scale bar: 100 μm. (C) Western-blot analysis shows the presence of endogenous, V5- and GFP-tagged Moe in both the nuclear (N) and cytoplasmic (C) protein fractions isolated from S2R+ cells. Beta-Tubulin (Tub) and HP1 antibodies were used as controls to exclude cross-contamination of the fractions. The panel shows the result of three western-blots, the whole blot images are shown in the supplementary material (Fig A.1). (D) Distribution of Moe-GFP (white) in the nucleus of a live salivary gland cell. Enlargement of the boxed region is shown to the right. White color – GFP signal, scale bar: 25μm.

Fig.2. The level of nuclear Moesin is tightly regulated. **(**A) Moe-GFP (white) accumulates in the nuclei of salivary gland cells after heat shock. The graph shows the ratio of nuclear/cytoplasmic fluorescence intensities in the nuclei of heat-shock treated salivary glands as compared to the untreated control. "n" refers to the total number of cells measured in 6 control animals and in 9 heat shocked animals. HS - heat shock. (B) Nuclear Moe level increases in salivary gland nuclei after 1h, 2h, and 3h treatment with an ecdysone hormone analog as compared to untreated nuclei. White color – Moe-GFP. (C) Moe level gradually increases in the nuclei of S2R+ cells after 15 and 30 min of heat-shock treatment. White color – Moe-GFP. Arrows point to nuclei. (D) Quantification of C. HS - heat shock. (E) Western-blot experiment demonstrating the increase in nuclear Moe protein level upon heat shock treatment of S2R+ cells. Beta-Tubulin (Tub) and HP1 antibodies were used as controls to exclude cross-contamination of the fractions. Numbers to the left indicate molecular weight in kDa. N – nuclear fraction, C - cytoplasmic fraction, HS – heat shock. Scale bars: 25 μm in A,D and 100 μm in B.

Fig. 3. Nuclear Moesin level is regulated by nuclear mRNA export. **(**A) Representative images of S2R+ cells expressing Moe-GFP and MAL-GFP (green) upon Nup98 and Rae1 knockdown and

stained with DAPI (blue). Optical sections were obtained via confocal microscopy and one mid-plane is shown. Quantified data are shown on the right. (B) Moe (magenta) accumulates in the nuclei of salivary gland cells depleted for Nup98. (C) Quantification of B. (D) Similarly to Moe, the mRNA export factor, PCID2, as well as Actin (green) accumulate in the nucleus upon Rae1 knock down. DAPI – blue. (E) Quantification of D. Scale bars: 25 μm in A, C and 100 μm in B. Graphs show the nuclear/cytoplasmic pixel intensity ratios, data represent mean rates +/- sd. *n* refers to the number of cells examined. n.s. – not significant.

Fig. 4. Moesin is involved in gene expression. (A-C) Endogenous Moe (A), and the Myc (B) and HA (C) epitope-tagged forms of the protein (magenta) have complementary distribution to DAPI staining (green) on giant polytene chromosomes. (D) Endogenous Moe protein (magenta) localizes to the puffs (encircled and white arrows) in the nucleus of untreated wild-type salivary glands as revealed by immuno-staining. Scale bar: 10μm. (E-F) Moe (magenta) accumulates to high-levels in the ecdysone (E) and heat-shock (F) puffs (encircled and white arrows). (G) Quantification of fluorescent intensity values of Moe-HA (magenta) and DAPI (green) stainings along the right arm of chromosome 3. (H) Triptolide treatment causes the dissociation of both RNA Polymerase II (Pol2 - green) and Moe (Moe-HA – magenta) from the giant polytene chromosomes. (I) Chromatin immunoprecipitation with Moe. Mean values of levels of HA tagged Moe precipitated of Drosophila *Act42a* and *Hsp70* gene regions in control (blue) and heat shock treated cells (red) are shown. HA tagged DTL protein precipitated of Drosophila *Act42a* and *Hsp70* genes in untreated cells (grey) was used as a control. Data are represented in percentage of total input chromatin content (input percentage). Error bars denote the standard deviations of the mean intensities of two independent measurements.

Fig. 5. Moesin is not involved in transcription initiation or termination. (A-B) Representative images of immunofluorescence staining of the chromosomes for Moe (magenta) and either the initiation-specific phosphoserine 5 (Pol2-PS5) (A) or the initiation+elongation-specific phosphoserine 2 (Pol2-PS2) (B) (green) forms of RNA Polymerase II. Arrows mark the double positive, and arrowheads mark the single positive bands. (C) Triple immunostaining for Moe, Pol2-PS5, and Pol2-PS2. Arrowheads point to a chromosome band in initiation phase, the arrows indicate an adjacent site of elongation phase while a double positive (PS5+PS2) site with very

strong initiation signal is labeled with an asterisk. (D) Quantification of fluorescent intensity values in C. (E) Recruitment of Moe (magenta) to the developing 74EF/75B ecdysone-induced puffs (arrows and arrowheads, respectively) and intermolt 68C locus (arrowheads) during development. Polytene chromosomes from larvae of different developmental stages (PS1-8) were stained with the Pol2-PS2 antibody (green) as control for transcriptional activity level. Blue – DAPI staining.

Fig. 6. Moesin is not involved in transcription, splicing or polyadenylation. (A) Immunofluorescent images of salivary gland cells treated with triptolide, DMSO or depleted for Moesin. 5-FUrd incorporation was applied as a measure of transcription and detected with anti-BrdU antibody. Scale bar: 100 μm (B) Quantification of 5-FUrd signal in A. (C) ePAT assay measuring poly(A) tail length of Hsp83 mRNA after heat shock induction in wild type (WT), hiiragi (hrg) or Moesin depleted larvae. The lengths of poly(A) tails are indicated. (D) Quantification of C. Arrows highlight the differences. The signal intensity of Hsp83 transcript was quantitated by the PlotLanes function of ImageJ. (E) In the salivary gland cell nucleus Moe (magenta) does not localize to SC35 splicing speckles (green). Arrows mark Moe foci in the nucleus. Enlargement of the boxed region is shown to the right. (F) Detection of spliced mRNA of Hsp83 (magenta) after heat shock induction in wild type and Moesin depleted salivary gland cells. Scale bars: 25μm.

Fig. 7. Moe is part of the mRNP complex. (A) In the polytene chromosome squash preparations Moe co-localizes with the mRNP particle components Rae1 and pAbp (arrows). (B) Co-immunoprecipitation control experiment showing the interaction between mRNA export factors Nup98-Myc (128.8 kDa) and Rae1-FLAG (41.64 kDa). (C) The V5 tagged PCID2 (46.62 kDa) protein pulled down both the FLAG tagged full-length Moe (Moe-FLAG, 70.94 kDa) and the GFP tagged FERM domain of Moe (FERM-Moe, 83.96 kDa). Numbers at left indicate molecular mass in kDa. IgGH – Heavy Chain of Immunoglobulin G. (D) The distribution of actin, the FERM (FERM-Moe) and the actin-binding (Act-Moe) domains of Moesin in the nucleus. White color – GFP signal, scale bar: 25μm. (E) Depolymerization of actin by Latrunculin A does not lead to the dissociation of Moe (Moe-HA – magenta) from the chromosomes.

Fig. 8. The depletion of Moesin impairs nuclear mRNA export. (A) Representative images of mRNA FISH experiments of S2R+ cells treated with Nup98 or Moe RNAi. Nuclear poly(A) level is elevated in these cells as compared to untreated cells (control). White color – FISH signal. Arrows mark the nuclei. (B) Representative images of mRNA FISH experiments on salivary glands treated with Nup98 RNAi, Leptomycin B (LMB) or Moesin RNAi. Nuclear mRNA level is increased in these cells as compared to that in untreated wild type glands (control). White color – FISH signal. (C) Quantification of the experiments in A and B. Graph shows the nuclear/cytoplasmic pixel intensity ratios measured in the nucleus and in the cytoplasm. Data represent mean rates +/- sd, *n* refers to the number of cells examined. Significance values were calculated with unpaired t-test. In the case of the salivary glands data were obtained in two independent experiments. Scale bars: 25 μm in A and 100 μm in B.

Fig. 9. Model depicting the nucleo-cytoplasmic transport and nuclear function of Moesin. Moe is incorporated during mitosis into the nucleus where it participates in mRNP complex formation and transport to the nuclear pore complex (NPC). Upon transcriptional activation or inhibition of mRNA export, the import of Moe is mediated by a yet unknown importin and, the protein level increases in the nucleus. During mRNA export Moe might dissociate from the mRNP particles at the NPC and remain in the nucleus. RNAPII – RNA Polymerase II, pAbp – polyA Binding Protein, Rae1 – RNA Export Factor 1, Nup98 – Nucleoporin98, NXF1 – Nuclear RNA export factor 1.

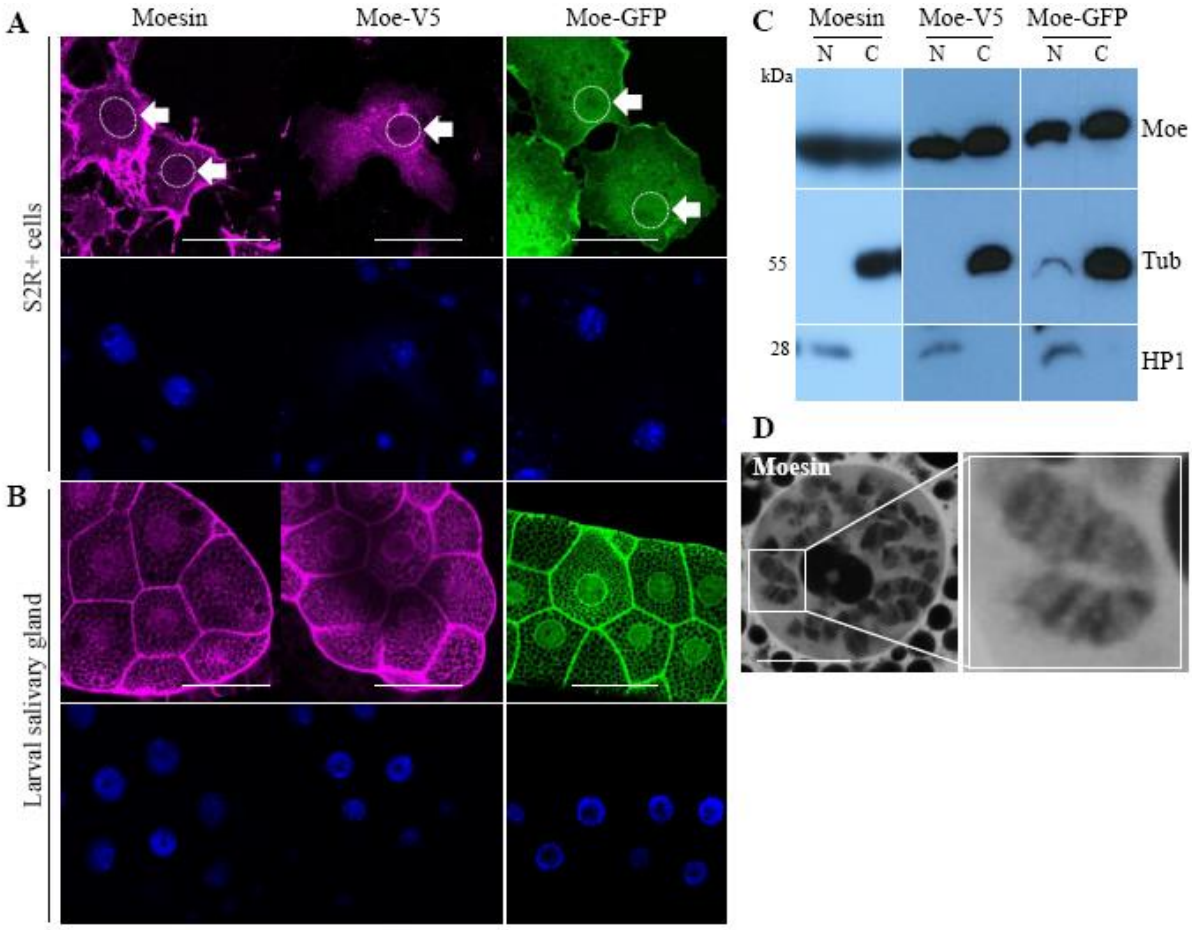

Figure 1

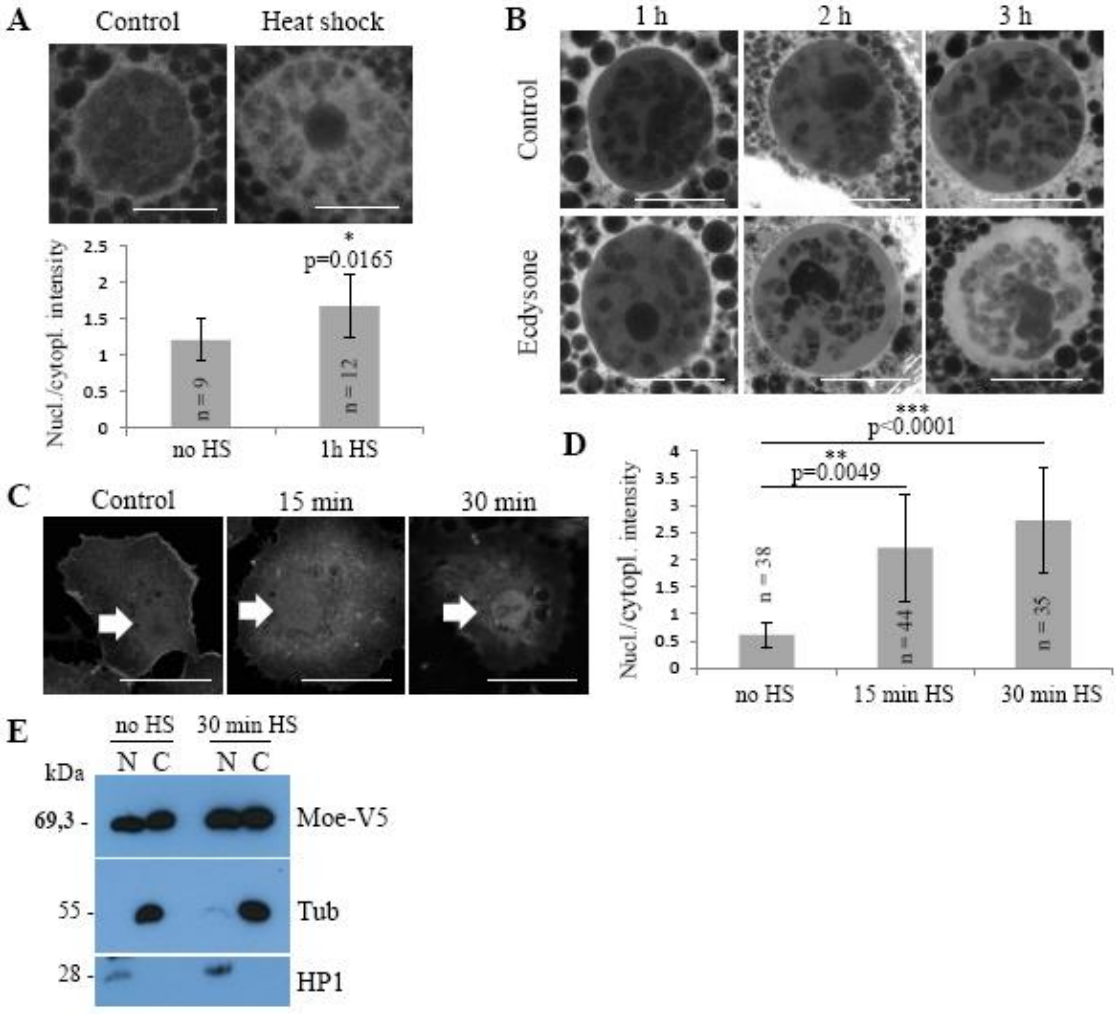

Figure 2

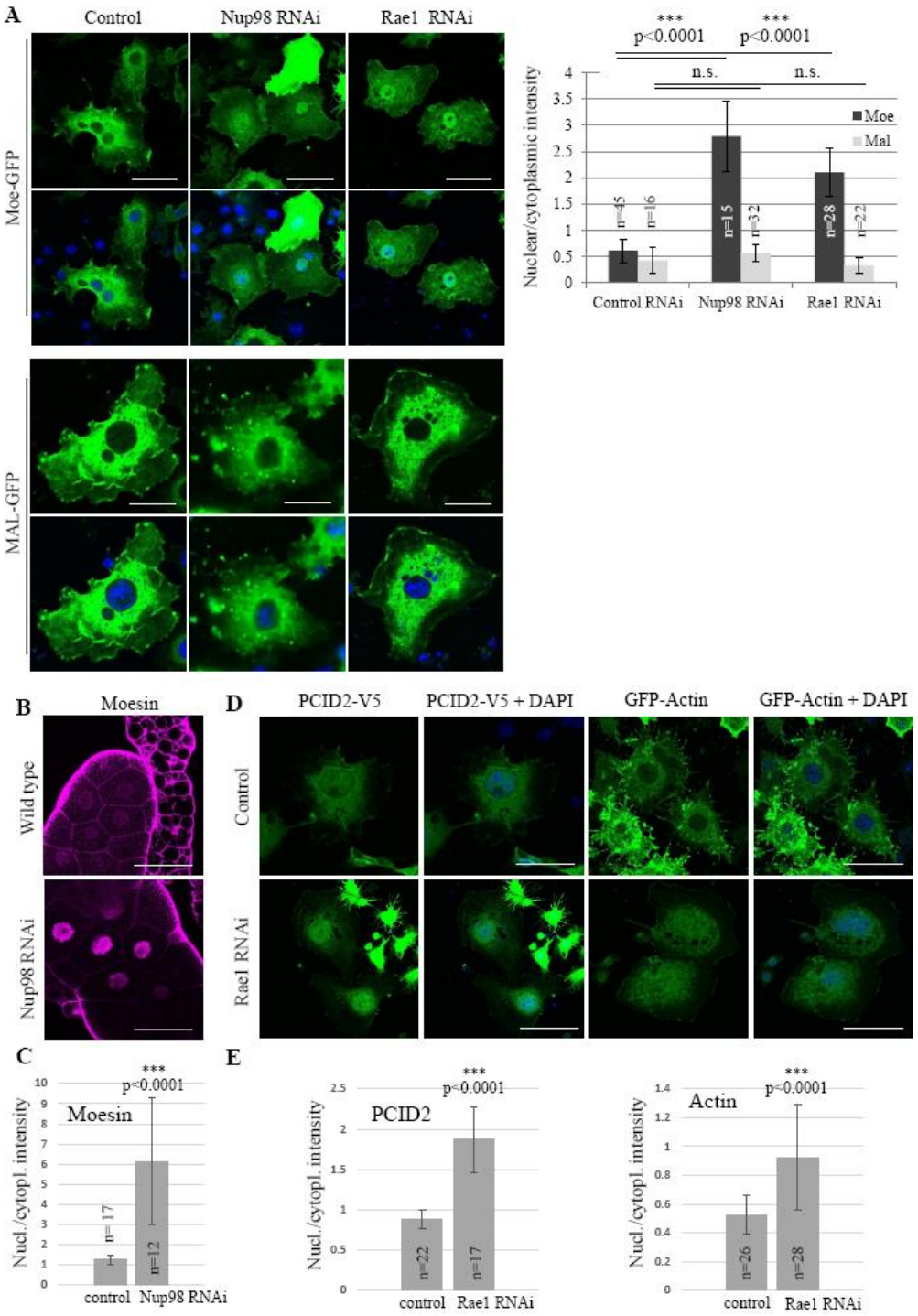

Figure 3

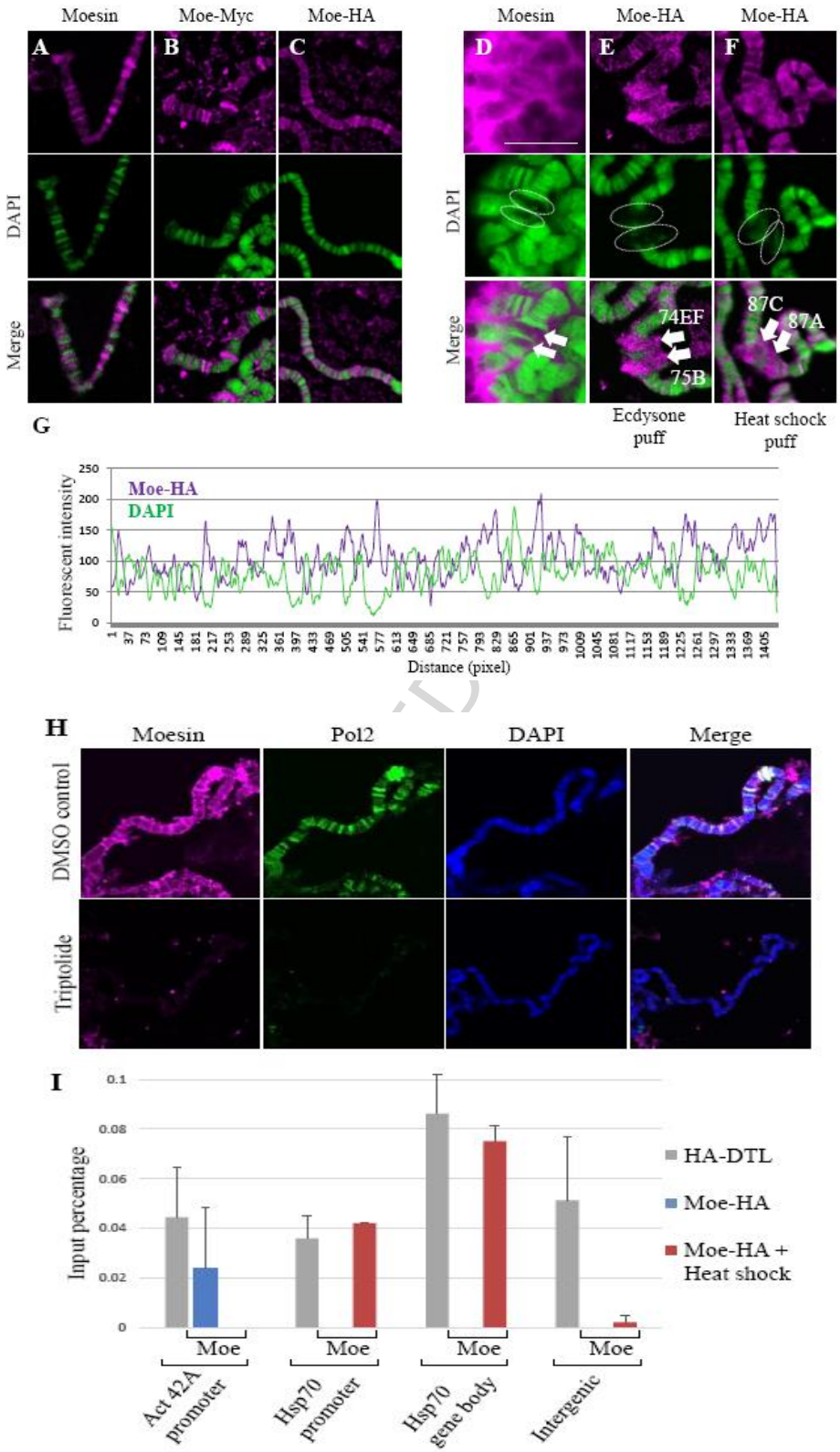

Figure 4

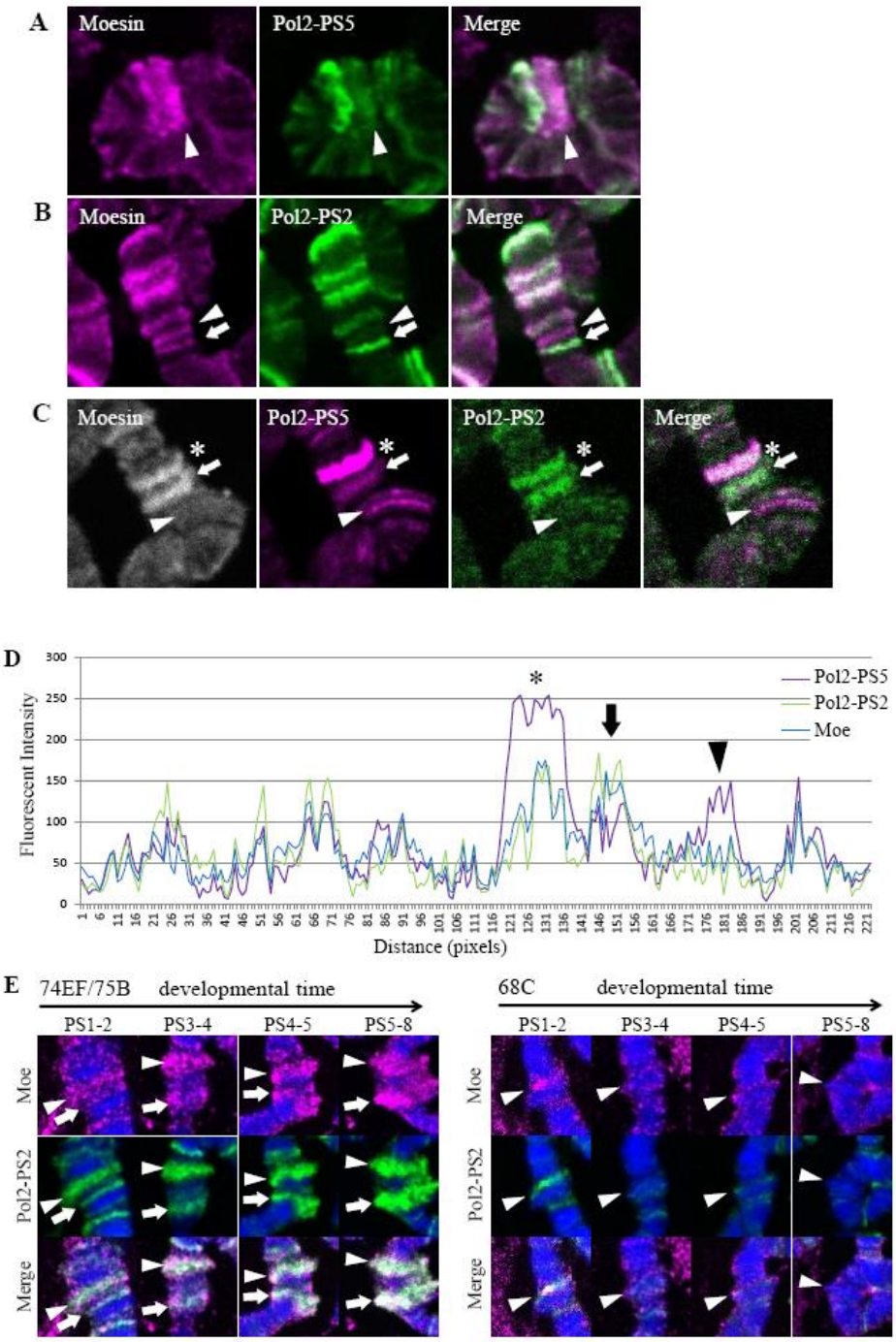

Figure 5

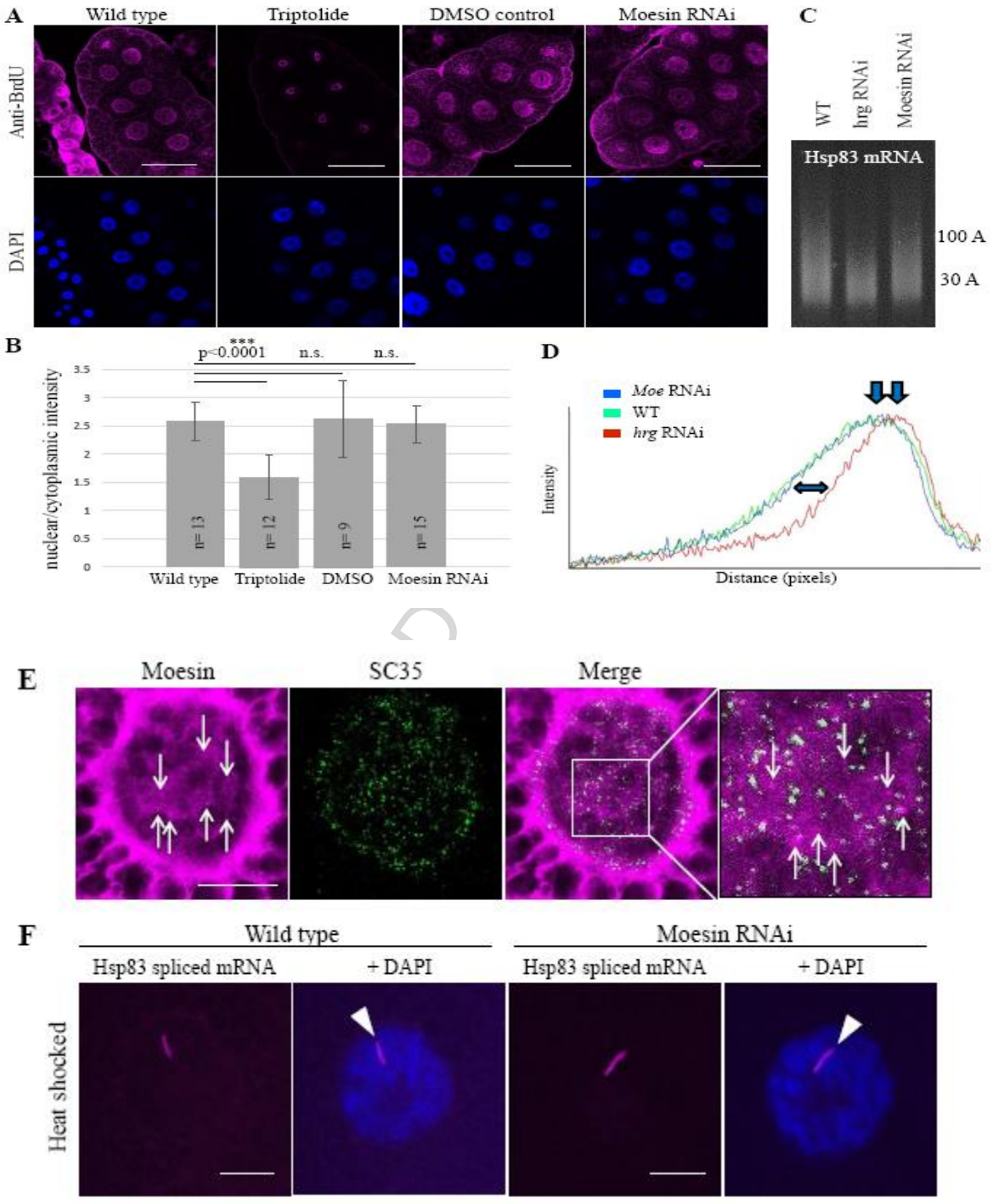

Figure 6

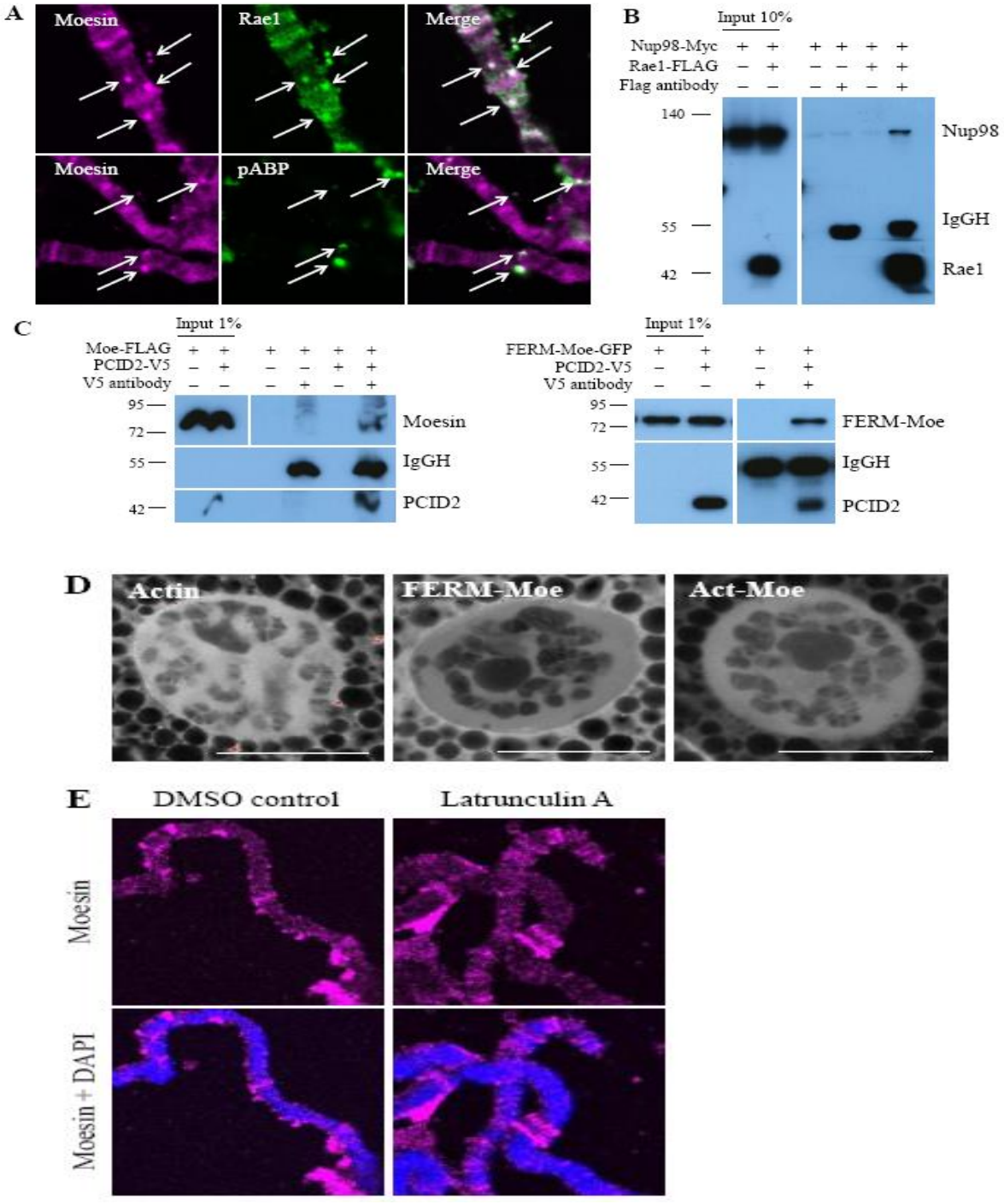

Figure 7

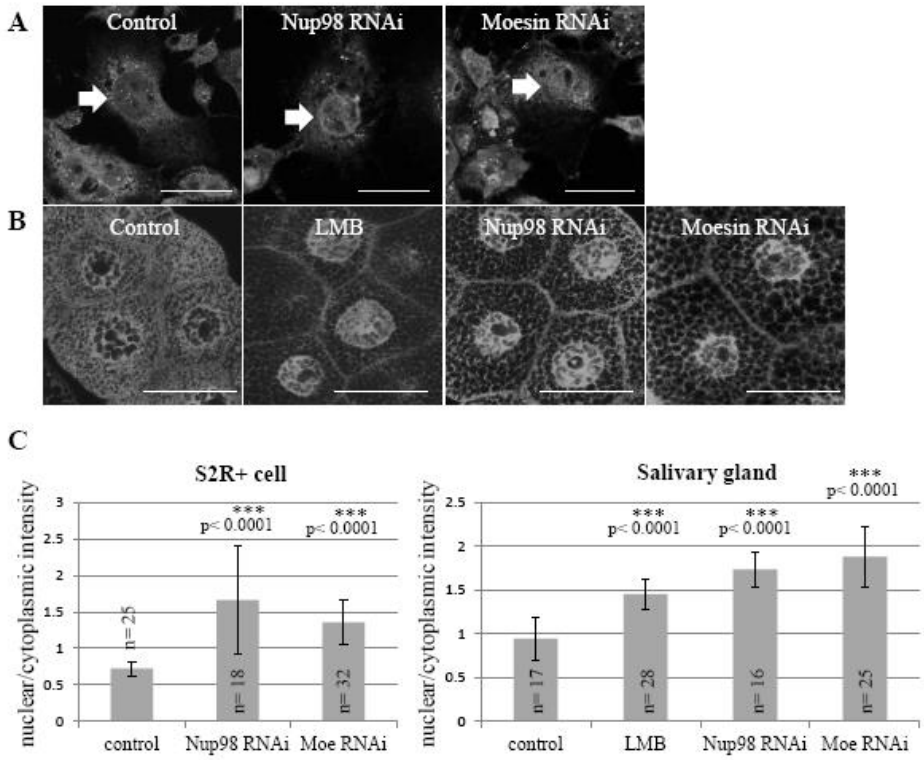

Figure 8

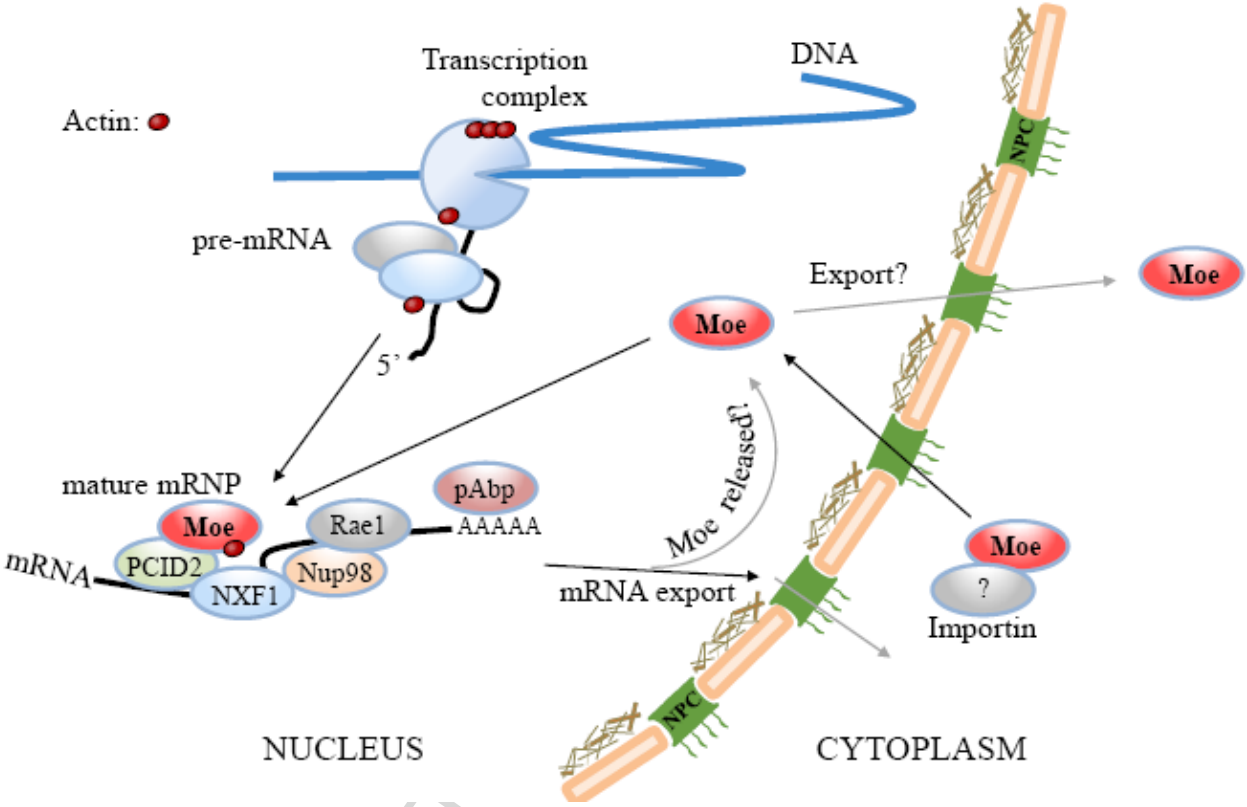

Figure 9

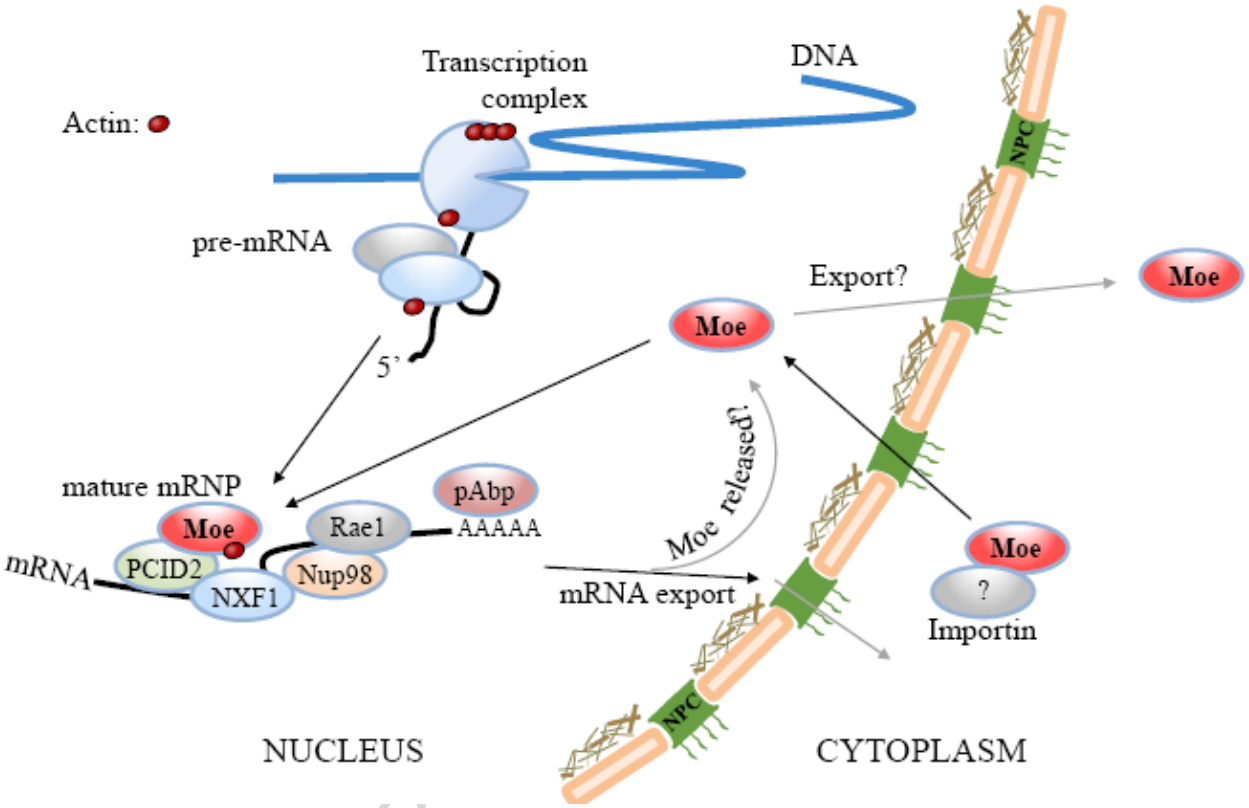

Graphical abstract

Highlights:

- The Drosophila Moesin protein is a functional component of the cell nucleus.
- In the nucleus Moesin participates in mRNA export.
- Moesin interacts with the mRNP complex member PCID2.